Journal of Energy Storage 48 (2022) 103983

Contents lists available at ScienceDirect

Journal of Energy Storage

journal homepage: www.elsevier.com/locate/est

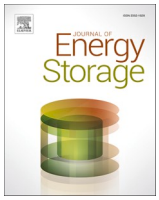

Research Papers

Adaptive Droop based Control Strategy for DC Microgrid Including Multiple Batteries Energy Storage Systems

Seydali Ferahtia [a,*], Ali Djerioui [b], Hegazy Rezk [c,d], Aissa Chouder [b], Azeddine Houari [e], Mohamed Machmoum [e]

[a] Laboratoire d'Analyse des Signaux et Systémes dept. of electrical engineering, University of M'sila, Algeria
[b] Laboratoire de Génie Electrique dept. of electrical engineering, University of M'sila, Algeria
[c] College of Engineering at Wadi Addawaser, Prince Sattam Bin Abdulaziz University, Saudi Arabia
[d] Faculty of Engineering, Minia University, Egypt
[e] IREENA Laboratory dept. of industrial engineering, University of Nantes, France

ARTICLE INFO

Keywords:
Droop control strategy
state of charge
battery storage
modern optimization
identification

ABSTRACT

In a microgrid architecture that includes energy storage systems based on parallel batteries, the inequalities in the batteries' state of charge may cause inconsistency in the residual capacity of each battery. As a consequence, the battery cells may be degraded owing to overcharging or deep discharging. This paper presents an optimized load-sharing approach-based droop control strategy for parallel batteries operating in a DC microgrid. The main aim of the proposed control approach is to include the real battery capacity, which may be affected during its lifecycle, in the control algorithm in order to prevent non-matching conditions. As a result, proportional power-sharing will be allowed according to the actual capacity. In addition, all the SoCs will be equalized and the parallel batteries, present in the system, will operate equally in terms of SoC when delivering or absorbing power. Hence, the batteries lifecycle will be extended while power-sharing is performed in the best way. To this end, the identification of the actual battery capacity has been carried out using a metaheuristic optimization algorithm called Salp Swarm Algorithm (SSA). Each battery output is controlled by bidirectional DC/DC converters that ensure the charging and discharging process. The control approach has been evaluated under different scenarios such as similar and different capacities and a sudden disconnection of a battery. The obtained results prove the ability of the proposed control strategy to ensure proportional power-sharing while handling the inconsistency of residual energy between battery cells and improve the battery state of health.

Introduction

Currently, with the increase of the energy crisis and greenhouse concerns; microgrid (MG) based power systems are becoming a promising solution [1]. MGs represent a combination of co-operating power sources. These sources include renewable energy sources (RESs), controllable sources such as fuel cells (FCs) and internal combustion engines (ICEs), energy storage systems (ESSs) and local loads [2,3]. MGs are equipped with supervisory control, protection and energy management systems [4,5]. The coordination of their operation is achieved using advanced power electronics converters [6]. MG technology is gaining more and more attention in many applications that have high consumption rates such as commercial buildings [7]. In general, most of RESs generates DC power which is compatible with ESSs and a large number of loads [8]. Based on these and other advantages, DC microgrids will dominate energy transmission and distribution in the near future. However, the integration of multiple power sources such as RESs, which are dependent on weather conditions, may lead to energy balance issues. For this reason, adding ESSs is required [9,10]. Integrating ESSs provides the system with a continuous power supply, higher reliability and resiliency [11].

It is well known that batteries baes ESSs have higher efficiency and a larger lifespan if their SoC is adequately maintained within their safe ranges [12]. However, in real cases, several factors may cause SoC unbalancing among paralleled batteries. These factors include initial SoCs, ESS capacity and line impedances [13]. It worth to mention here that the SoC imbalance accelerates the discharge rate of the weak battery, and as a result, reduces its lifetime. Thus, it is of prime interest, in terms of SoC balancing to control the charging/discharging process in an

* Corresponding author:Dr. Seydali Ferahtia, University of M'sila, Universite de M'sila, Algeria
E-mail address: sidali.ferahtia@univ-msila.dz (S. Ferahtia).

https://doi.org/10.1016/j.est.2022.103983
Received 19 September 2021; Received in revised form 30 November 2021; Accepted 5 January 2022
Available online 10 January 2022

Nomenclature

MG	Microgrid
ESS	Energy storage system
RES	Renewable energy source
MG	Microgrid
SoC	State of charge
SoH	State oh health
V_{batt}	The battery voltage
i_{batt}	The battery current
V_{OC}	The open-circuit voltage
Q	The battery capacity
R_{int}	The battery internal resistance
k_d	Droop compensation factor
α	Convergence factor
V_{ref}	The common bus reference voltage
$V_{estimated}$	The model output voltage
R_{load}	The load resistance
MA	Metaheuristic algorithm
SSA	Salp Swarm Algorithm

adequate way to guaranty proportional power-sharing [14,15].

In the literature, microgrid control strategies can be generally classified as centralized, decentralized, and distributed [16]. The centralized control strategy is based on one central controller that generates the power reference of each power source [17]. In the case of a decentralized control strategy, each source operates with its sensors and local controller. For the distributed control strategy, serval controllers communicate between them to decide the operating state of the power system. For instance, centralized SoC balancing strategies are proposed in [18,19]. The proposed methods require communication lines and a central controller. The main drawback of the proposed strategies is the venerability and high installation costs due to the presence of the communication lines. A distributed control strategy is proposed in [20] in order to balance the SoC. A similar strategy is proposed in [21]. These strategies may provide high reliability. Nevertheless, it required large communication network. Decentralized methods which no communication lines such as droop control methods remain the most effective methods for this kind of application [22]. The author in [23] proposed modified droop coefficients as a function of the ESS's SoC. Different droop coefficients are chosen and their power-sharing speed rate is investigated based on the small-signal model. Another work proposed in [24] presents a different droop control method based on voltage scheduling to balance the SoC of different ESSs by adjusting voltage references. This strategy can resolve the stability issues that existed in conventional strategies based on droop gain scheduling. An intelligent droop coefficients scheduling based on fuzzy logic is proposed in [25]. The fuzzy logic controller updates the value of the virtual resistance according to the ESS' SoC. This strategy guarantees the SoC balancing among ESSs as well as reduced voltage deviation. Master-slave based consensus algorithm with pinning node is presented in [14]. Active SoC balancing based on the average state of charge and the battery charging/discharging state is proposed in [26]. The balancing will be performed according to the charging/discharging process. The paper presents a SoC estimation algorithm based on an extended Kalman filter. Hybrid droop and multi-agent sliding mode control strategy for SoC balancing is presented in [27]. The main advantages of this strategy are reducing circulating currents, improving efficiency and avoiding battery

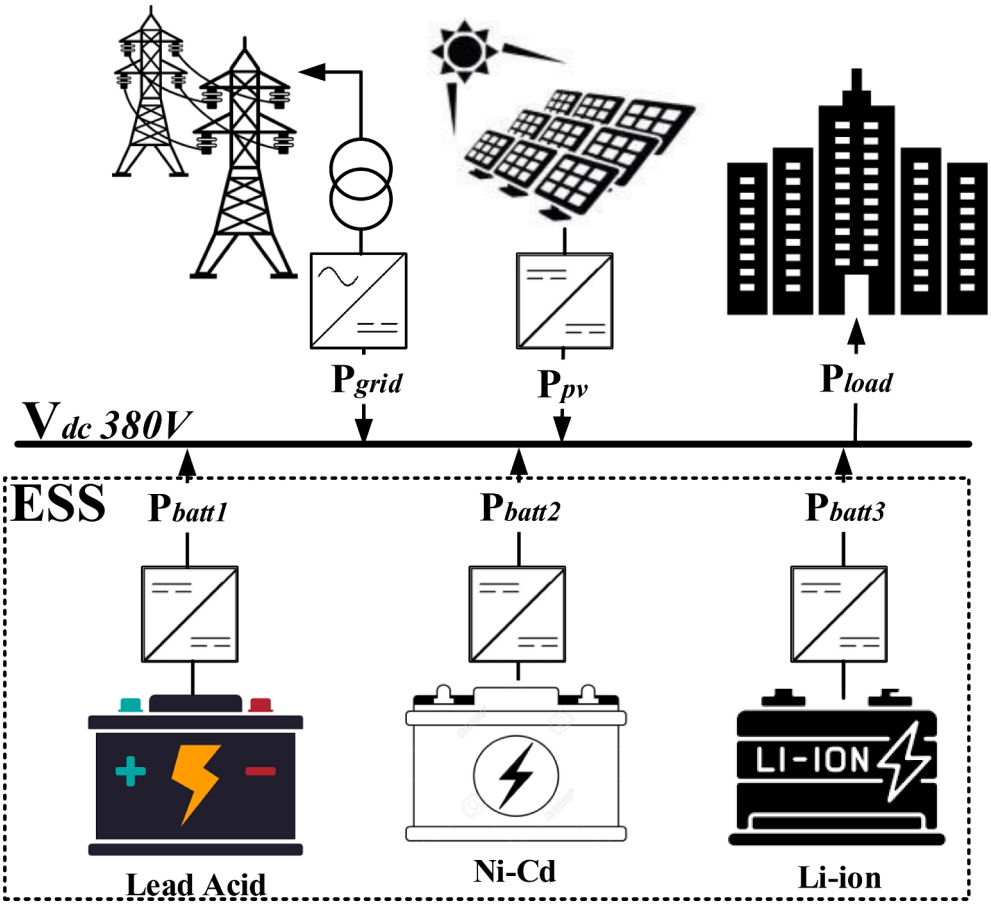

Fig. 1. The proposed DC microgrid Architecture includes the energy storage system (ESS), the loads, the PV array and the main grid connector.

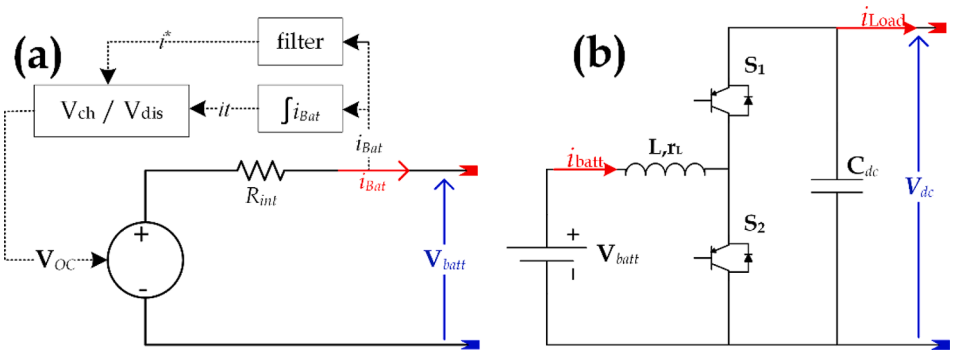

Fig. 2. Elements topology: a- Rint battery equivalent circuit model (ECM), b- Bidirectional Boost Converter.

overloading. A modified virtual resistance based on the battery SoC to update the droop control strategy is proposed in [28]. This strategy controls the balancing speed by adjusting the exponent of SoC in the proposed control strategy. An intelligent fuzzy-based droop control strategy is presented in [29], where the fuzzy controller updates the droop control parameters. The key advantage of this strategy is its performance with unknown or complex models. However, the accurate design of the fuzzy controller is difficult. However, all the previous methods are based on prior knowledge of the ESS parameters such as the capacity. In fact, because of their chemical characteristics, batteries are gradually degrading by the ageing effect [30]. A deep learning-based artificial neural network for SoC balancing considering the state of health is proposed in [31]. However, the complexity of this strategy is relatively high and data to train the estimation model. Instead of SoC balancing, droop control for SoH balancing is proposed in [32]. This strategy includes only the SoH in the control strategy, where the SoC is not included, moreover, the SoH variations is very slow compared with the SoC variations. SoC balancing based model predictive control (MPC) that includes the states such as temperature and state of charge is proposed in [33]. The thermal balancing may restrict the battery degradation; however, the battery capacity did not include; in addition, the MPC based control strategy is very complex.

Motivation and contribution

Since the conventional droop control strategy does not take into account the actual value of the capacity, it may reduce its state of health (SoH) faster. For this reason, the identification and the consideration of the actual capacity are required to avoid premature ageing. In this paper, the main aim of the proposed control approach is to include the real battery capacity, which may be affected during its lifecycle, into the control algorithm in order to prevent the non-matching conditions and therefore allow proportional power-sharing according to the actual capacity. As a result, the state of charge will be matched and all parallel batteries, present in the system, will be equalized in terms of SoC. Hence, the batteries lifecycle will be extended while power-sharing is performed in the best way. To this end, the identification of the actual battery capacity has been performed using a metaheuristic optimization algorithm called Salp Swarm Algorithm (SSA). Each battery output is controlled by a bidirectional DC/DC converters that ensure the charging and discharging process. Battery parameters identification based on metaheuristic algorithms is gaining more attention due to their high performance and simplicity [34]. Because of its significant advantage, the salp swarm algorithm (SSA) [35] is used to estimate the real battery's capacity. The droop coefficients are thus updated according to the obtained results by the optimizer.

The rest of the paper is organized as follows; Part 2 explains the proposed power system configuration including the models. Part 3 discusses the droop control strategy including the PI controller. The battery state of health estimation algorithm is proposed in Part 4. The results are discussed in Part 5. This paper ends with a conclusion and future works.

System Configuration and Modeling

The proposed power system is based on a grid-connected DC microgrid, which is composed of a combined solar PV array and energy storage system (ESS). The power system topology is given in Fig. 1. The ESSs are connected to the common bus (380V) in parallel. Each one shares its power based on the droop control strategy. The other sources including the load are considered as bidirectional current sources.

Li-ion batteries are currently the most used batteries even with their high cost. They provide superior performance over the other types such as lifespan, energy density, and response time. Based on Shepherd Relation [36,37] the Li-ion battery discharging equation can be written as

$$V_{dis} = V_{OC} - \frac{Q}{Q-it} - R_{\text{int}}.i + A.e^{(-B^*it)} - K\frac{Q}{Q-it}i^* \tag{1}$$

where V_{dis} denotes the battery output voltage during the discharging phase (V). V_{OC} is the battery constant voltage (open circuit voltage). Q is the battery capacity (Ah). K is a polarization constant (V/Ah) or polarization resistance (Ω). it is the actual battery charge ($it = \int idt$) (Ah). A is the exponential zone amplitude (V). B is the exponential zonetime constant inverse (Ah^{-1}). R_{int} is the internal resistance (Ω). i and i^* are the battery current and the filtered current respectively (A).

According to the internal resistance model [38,39] (Fig. 2 (a)), the battery voltage can be expressed as a function of the battery open-circuit voltage (V_{oc}) and the internal resistance (R_{int}) as follow

$$V_{batt} = V_{OC}(SoC) - R_{\text{int}}(SoC, T)i_{batt} \tag{2}$$

where V_{batt} and i_{batt} are the battery voltage and current, SoC is the battery state of charge and T is the operating temperature. According to [40], V_{OC} and R_{int} can be calculated as a function of the state of charge as follow

$$X = a_0 + a_1SoC + a_2SoC^2 + a_3SoC^3 + a_4SoC^4 + +a_5SoC^5 + a_6SoC^7 + a_7SoC^7 \tag{3}$$

where a_0, a_1, a_3, a_4, a_5, a_6 and a_7 are model parameters and X is the model variable (V_{OC} and R_{int}).

The battery SoC can be estimated as follow.

$$SoC(t) = SoC_0 - \frac{1}{Q}\int i_{batt}dt \tag{4}$$

where SoC(t) is the battery state of charge, SoC_0 is the initial SoC.

A bidirectional boost converter (BBC) is used to control the battery output power; its topology is represented in Fig. 2(b). The BBC is used to charge the battery (buck mode) using the bus power or to supply the bus by injecting battery power (boost mode). The BBC is controlled by the duty ratio d. The model of BBC can be described as

Table 1
BBC transfer functions.

	Buck	Boost
Voltage TF $\frac{V_{dc}}{d}$	$V_{batt}\frac{R_{load}}{s^2LC_{dc}R_{load}+sL+R_{load}}$	$\frac{V_{batt}}{(1-D)}\frac{(1-D)^2R_{load}-sL}{s^2LC_{dc}R_{load}+sL+R_{load}}$
Current TF $\frac{I_L}{d}$	$V_{batt}\frac{1+sC_{dc}R_{load}}{s^2LC_{dc}R_{load}+sL+R_{load}}$	$\frac{V_{batt}}{(1-D)}\frac{2-sC_{dc}R_{load}}{s^2LC_{dc}R_{load}+sL+R_{load}}$

Where R_{load} is the load resistance and $C_{dc} = C_o$.

$$\begin{cases} L\frac{di_L}{dt} = v_i - (1-d)v_o i_{batt} \\ C_o\frac{dv_o}{dt} = (1-d)i_L - i_o \end{cases} \quad (5)$$

where v_i and v_o are the input and output voltages, i_L is the inductor current, i_o is the output current flowing into the dc bus, L is the inductance, and C_o is the converter output capacitance. Based on the small-signal model, the converter transfer functions are given in Table 1.

Proposed Control Strategy

SoC balancing method

The proposed control strategy is based on the droop control approach. This method allows each power source to control its own power locally. Fig 3 represents the V-I droop characteristics of two different batteries, from this figure, to control the battery output voltage at the reference bus voltage ($V_{batt} = V_{bus}$), the output current must be maintained at the suitable value I_{batt}. The current value is defended according to the virtual resistance (R_{vb}) as described in Eq. (6)

$$V_{batt} = V_{oc} - R_{Vb}i_{batt} \quad (6)$$

The Droop control forces the batteries to provide the currents i_{batt1} and i_{batt2} so that $V_{batt1} = V_{batt2} = V_{bus}^{ref}$, but the SoC balancing problem has yet to be resolved. Several methods have been presented in the literature review that includes the SoC in the control low. Adaptive droop compensation functions for SoC balancing have been reported in [41], the modified droop function can be written as follow

$$V_{batt} = V_{oc} - k_d(SoC, \alpha)R_{Vb}.i_{batt} \quad (7)$$

where k_d is the compensation function and α is the droop factor; these functions are presented in Table 2.

The used method is based on the combination of the SoC with droop control, the modified droop equation becomes:

$$V_{batt} = V_{oc} - R_{Vb}.i_{batt} + \alpha.SoC \quad (8)$$

where α is the droop factor which determines converges speed.

The battery reference voltage can be written as

$$V_{ref} = V_{oc} + \alpha.SoC \quad (9)$$

$$V_{bus} = V_{ref} - R_{Vb}.i_{batt} \quad (10)$$

Balancing speed

From Eq. (4), the balancing speed can be exposed as a function as the SoC variation, as follow

$$v = \frac{dSoC}{dt} = -\frac{i_{batt}}{Q} \quad (11)$$

The balancing speed between two batteries can be written as

Table 2
BBC transfer functions.

Function	Compensation function k_d	
	Discharging	Charging
Linear	$\alpha(1-SoC)+1$	$\alpha^{-1}(SoC-1)+1$
Power	SoC^{α}	$SoC^{-\alpha}$
Exponential	$e^{-\alpha(SoC-1)}$	$e^{\alpha(SoC-1)}$
Hyperbolic Sine	$\sinh(-\alpha(SoC-1))+1$	$\sinh(\alpha^{-1}(SoC-1))+1$
Logarithmic	$-\alpha.\ln(SoC)+1$	$\alpha^{-1}.\ln(SoC)+1$

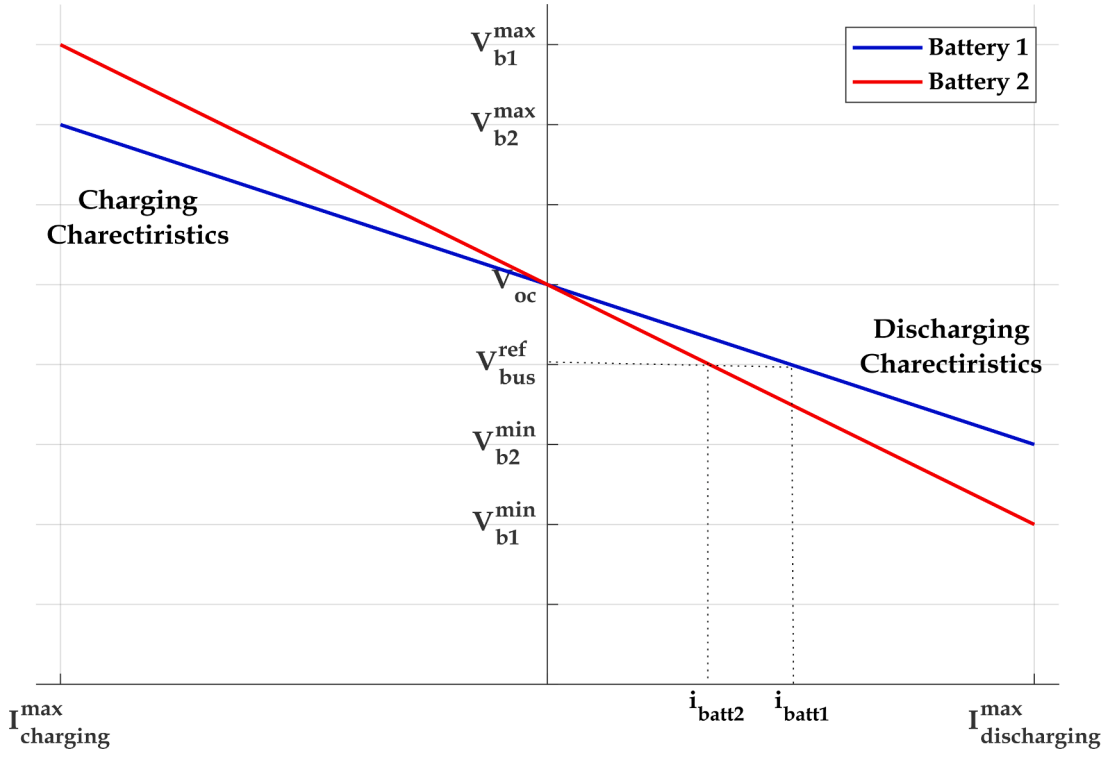

Fig. 3. V-I droop characteristics of two distinguished batteries.

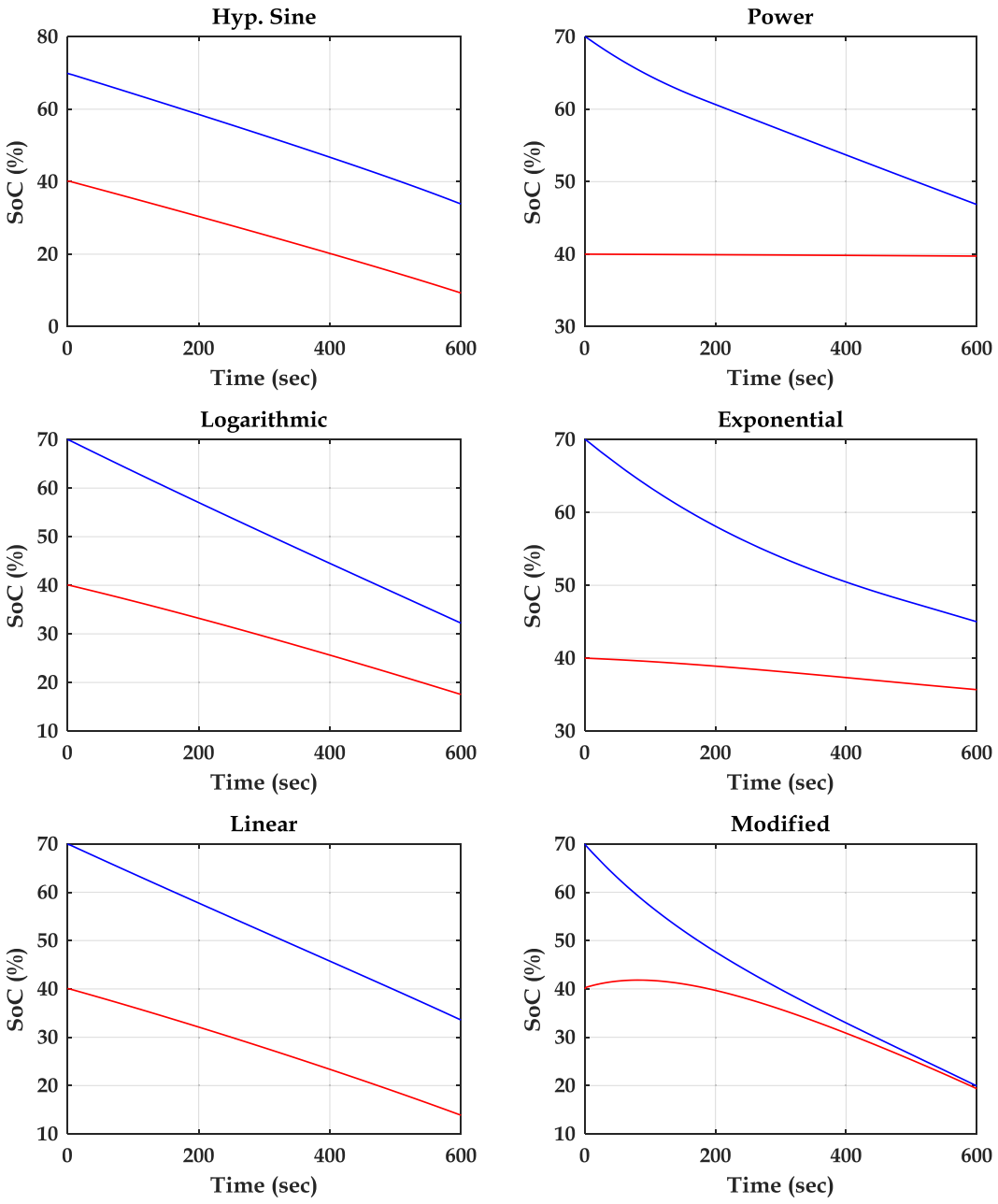

Fig. 4. Balancing results of each strategy.

$$v_1 - v_2 = -\frac{i_{batt1}}{Q_1} - \left(-\frac{i_{batt2}}{Q_2}\right) \tag{12}$$

From Eq. (10), the battery current can be expressed as

$$i_{batt} = \frac{V_{ref} - V_{bus}}{R_{Vb}} \tag{13}$$

Thus, the current of batteries 1 and 2 and the bus can be expressed as

$$i_{batt1} = \frac{V_{ref1} - V_{bus}}{R_{b1}} \tag{14}$$

$$i_{batt2} = \frac{V_{ref2} - V_{bus}}{R_{b2}} \tag{15}$$

$$i_{bus} = \frac{V_{bus}}{R_{load}} = i_{batt1} + i_{batt2} = \frac{V_{ref1} - V_{bus}}{R_{b1}} + \frac{V_{ref2} - V_{bus}}{R_{b2}} = \frac{R_{b1}\left(V_{ref2} - V_{bus}\right) + R_{b2}\left(V_{ref1} - V_{bus}\right)}{R_{b1}R_{b2}} \tag{16}$$

The bus voltage can be written as

$$V_{bus} = i_{bus}R_{load} = \frac{R_{b1}\left(V_{ref2} - V_{bus}\right) + R_{b2}\left(V_{ref1} - V_{bus}\right)}{R_{b1}R_{b2}}R_{load} \tag{17}$$

The output power of each battery is

$$P_{batt} = i_{batt}V_{ref} = \frac{\left(V_{ref} - V_{bus}\right)}{R_b}V_{ref} \tag{18}$$

Replacing the value of V_{bus} Eq. (17) on Eq. (18) and following the same steps with [42,43], the output power and the power difference between the batteries if $R_1 = R_2 = R$, they can be written as

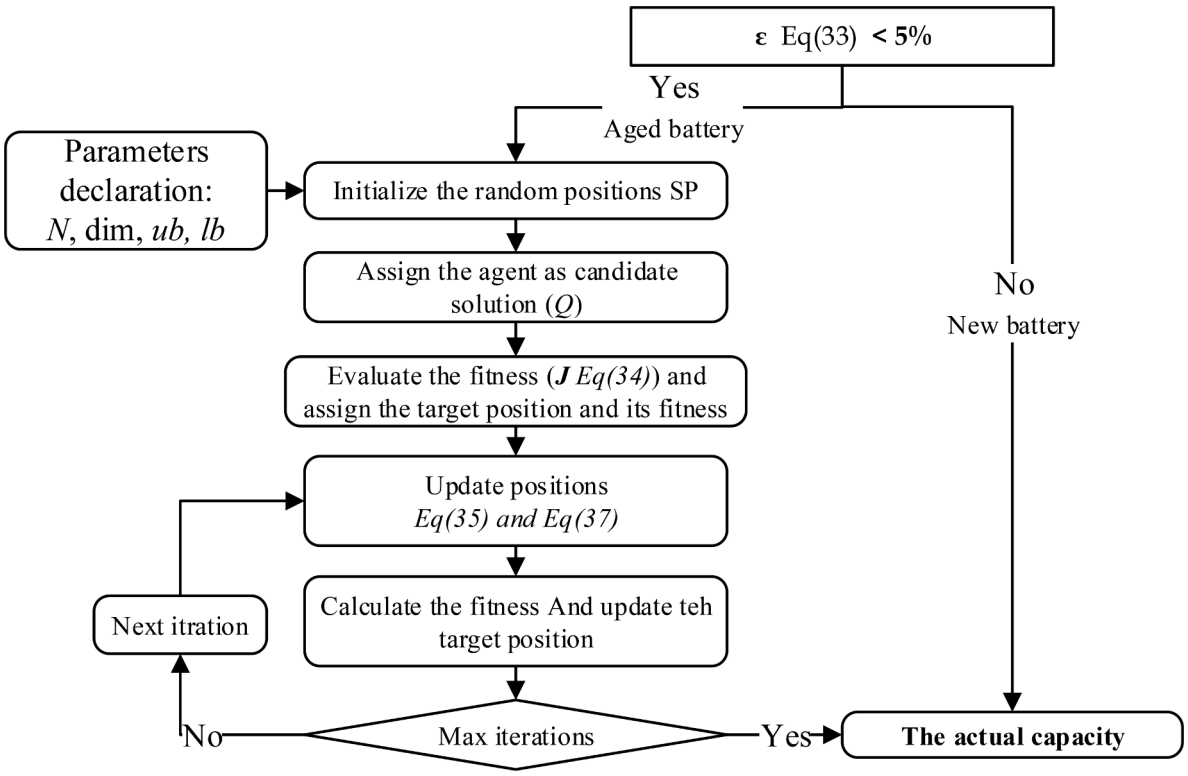

Fig. 5. Flowchart that expresses the battery observatory and the identification algorithm.

$$P_{batt1} = (V_{oc} - \alpha SoC_1)\frac{SoC_1(R + R_{load})\alpha - \alpha R_{load} SoC_2 + RV_{oc}}{R(2R_{load} + R)} \tag{19}$$

$$P_{batt2} = (V_{oc} - \alpha SoC_2)\frac{SoC_2(R + R_{load})\alpha - \alpha R_{load} SoC_1 + RV_{oc}}{R(2R_{load} + R)} \tag{20}$$

$$\Delta P = \frac{\alpha(SoC_1 - SoC_2)(R + R_{load})(2V_{OC} + \alpha(SoC_1 + SoC_2))}{R(2R_{load} + R)} \tag{21}$$

If the batteries are identical, the balancing speed express in Eq. (12), it can be rewritten as

$$\begin{aligned} v_1 - v_2 &= -\frac{P_{batt1}}{V_{batt1}Q_1} + \frac{P_{batt2}}{V_{batt2}Q_2} = \frac{\Delta P}{V_{batt}Q} \\ &= \frac{\alpha(SoC_1 - SoC_2)(R + R_{load})(2V_{OC} + \alpha(SoC_1 + SoC_2))}{V_{batt}.Q.R.(2R_{load} + R)} \end{aligned} \tag{22}$$

If the batteries have deferent capacities, Eq. (12) can be presented as

$$v_1 - v_2 = -\left(\frac{V_{batt1}}{R_{Vb1}Q_1} - \frac{V_{batt2}}{R_{Vb2}Q_2}\right) \tag{23}$$

To balance the SoC, Eq. (23) must be equal to zero, thus, if the batteries have to provide the same output voltage, the virtual resistances have to be set as

$$R_{Vb1} = \frac{R_{Vb2}Q_2}{Q_1} \tag{24}$$

For a storage system with three batteries, the virtual resistance have to be set as follows

$$R_{Vb2} = \frac{R_{Vb3}Q_3}{Q_2} \tag{25}$$

$$R_{Vb1} = R_{Vb2}\frac{Q_2}{Q_1} = \frac{R_{Vb3}Q_3}{Q_1} \tag{26}$$

Droop factor limitation speed

Although a large droop factor could increase the SoC balancing speed, there are some constraints on its selection including the bus voltage control, the battery current limits, and the transmission power limits.

Bus voltage control constraints

The bus voltage must be maintained within its allowable range $\pm u$ %, thus, the droop factor at SoC = 100% has the following constraint

$$\alpha + i_{charging}^{\max} R < uV_{ref} \tag{27}$$

Battery current limits

The battery output power have to be lower than the maximum one, thus, the droop factor have the following constraint

$$\alpha < ((R_{load} + R)i_{\max} - V_{batt}) \tag{28}$$

As demonstrated in the previous analysis, the droop control strategy is based on battery capacity. Thus, the real capacity value will be updated by means of the updating mechanism.

Fig. 4 shows the balancing results of each strategy, the testing was for two batteries. From these results, the balancing speed using the modified droop control strategy is much better than the other reported strategies.

PI controller designing

The PI controller has been designed based on the transfer function (TF) of the converter that is provided in Table 1. The TF on the open-loop can be written as

$$T_{vd}(s) = T_0\frac{1 - s/\omega_z}{1 + s/\xi\omega_0 + s^2(s/\omega_0)^2} \tag{29}$$

where

$$\begin{aligned} T_0 &= \frac{V_{batt}}{(1 - D)}; \qquad \xi = (1 - D)R_{load}\sqrt{C_{dc}/L} \\ \omega_z &= (1 - D)R_{load}/L; \qquad \omega_0 = (1 - D)\Big/\sqrt{LC_{dc}} \end{aligned} \tag{30}$$

Based on the control law proposed in [44], the PI controller parameters can be calculated as follow

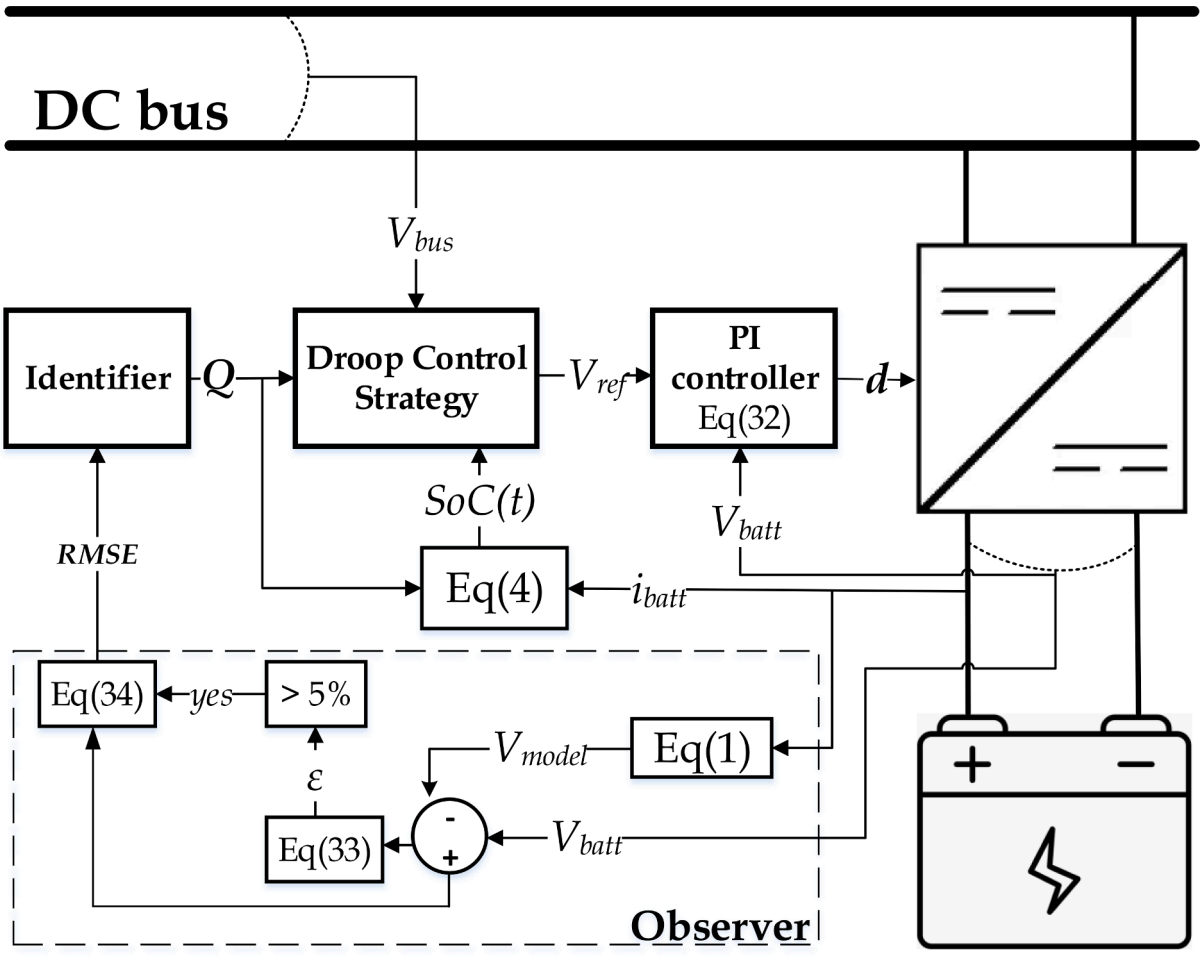

Fig. 6. The global operating scheme of the proposed control strategy includes the battery observation and identification algorithm, the modified droop control block and duty cycle generation block based on the PI controller.

Table 3
Simulation parameters.

Parameters	Value
Bus voltage reference	380 V
SoC_{01}	80 (%)
SoC_{02}	60 (%)
SoC_{03}	40 (%)
A	0.22
R	0.1 Ω
R_{load}	5 k Ω
C	0.001 H
L	0.001 F

$$k_p = \frac{1}{|T_{vd}(s)|}$$
$$ki = 2\pi f_c \frac{k_p}{10} \quad (31)$$

where f_c is the cutoff frequency. The PI controller TF is written as follow

$$C_{PI}(s) = k_p + \frac{k_i}{s} \quad (32)$$

Battery capacity identification strategy

The proposed droop control method is mainly based on the capacity of the battery Q. This method applies to batteries that their Q is known. However, if one of the used batteries is aged, the power-sharing will be unbalanced. And therefore, the batteries lifecycle will be reduced. For this, the battery state of health (SoH) should be identified.

The identifier is turned on by means of the observer. The observer compares the battery output voltage and the output model if the error is greater than 5%, the identifier is switched on. The error is defined as follows

$$\varepsilon = \frac{V_{batt} - V_{model}}{V_{batt}}.100 \quad (33)$$

where V_{bat} is the battery voltage, V_{model} is the battery model output that is defended in Eq. (1).

In this paper, the identification method is used to determine the actual capacity. This method is based on the salp swarm algorithm (SSA) [35]. SSA is a stochastic metaheuristic algorithm (MA), this characteristic allows the algorithm to converge toward the global optima and prevent attempting on the local optima. As a MA, this algorithm starts from random solutions. These solutions will be updated according to the best-obtained result in the previous iteration and according to the SSA updating mechanism.

A battery model based on Eq. (1) is used as a reference, where the only unknown parameter is Q. The optimizer tends to minimize the voltage error between the model and the real data.

In each iteration, the agents move toward the target (the actual Q), where the objective function is to minimize the root main square error (RMSE) between the model output voltage and the battery measurements

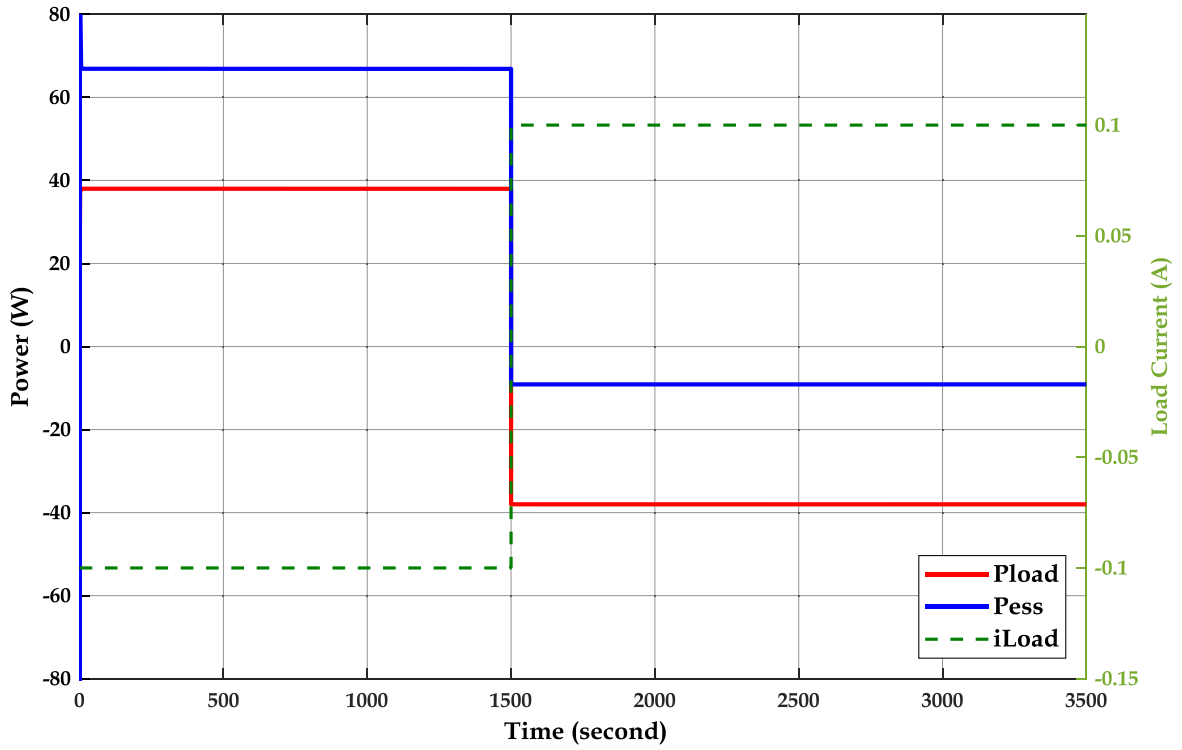

Fig. 7. The Load Current and Power and the ESS Power.

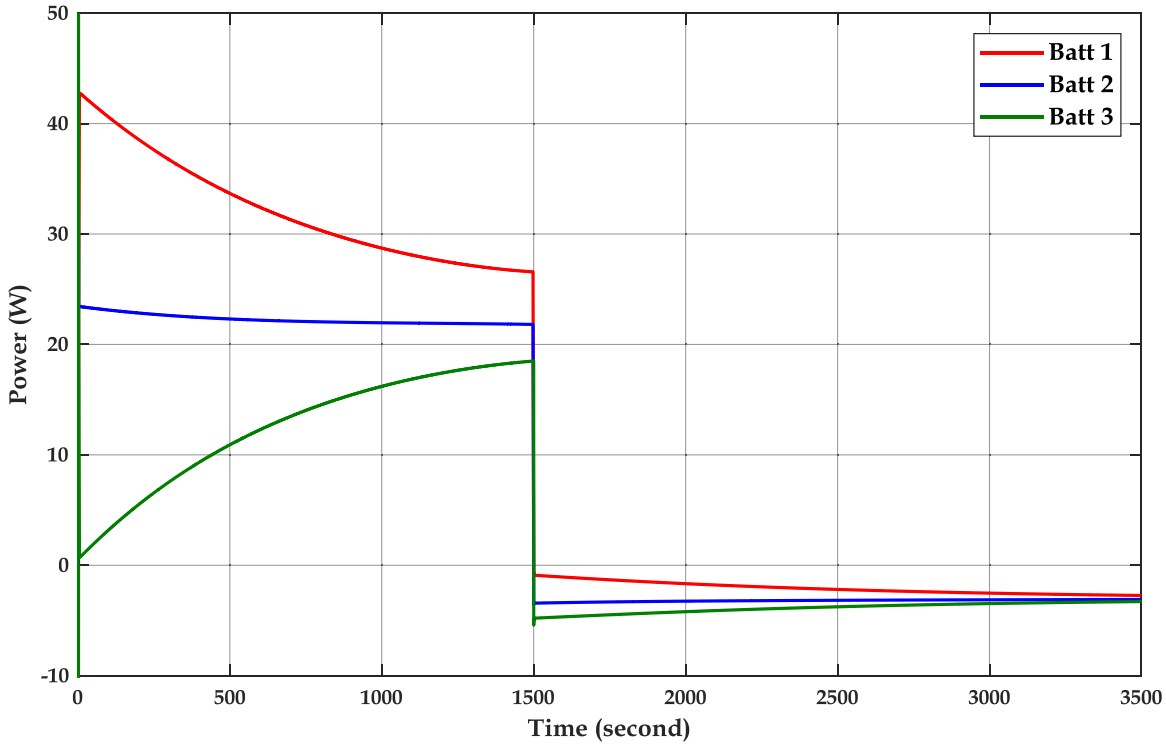

Fig. 8. Power-sharing with the proposed droop strategy.

$$J = \min\left(\sqrt{\frac{1}{T}(V_{batt} - V_{estimated})^2}\right) \tag{34}$$

The first step is to initialize the population, each agent from this population is a candidate solution. The value of each agent is assigned as the actual capacity and the simulation runs with this value. The RMSE will send back to the optimizer as a fitness of the candidate solution and the optimizer will update the best position according to these results. The simulation runs again with the newly updated positions. According to the obtained fitness, the optimizer updates the position of his agents and evaluates the fitness of the new positions. This process will repeat until the last iteration.

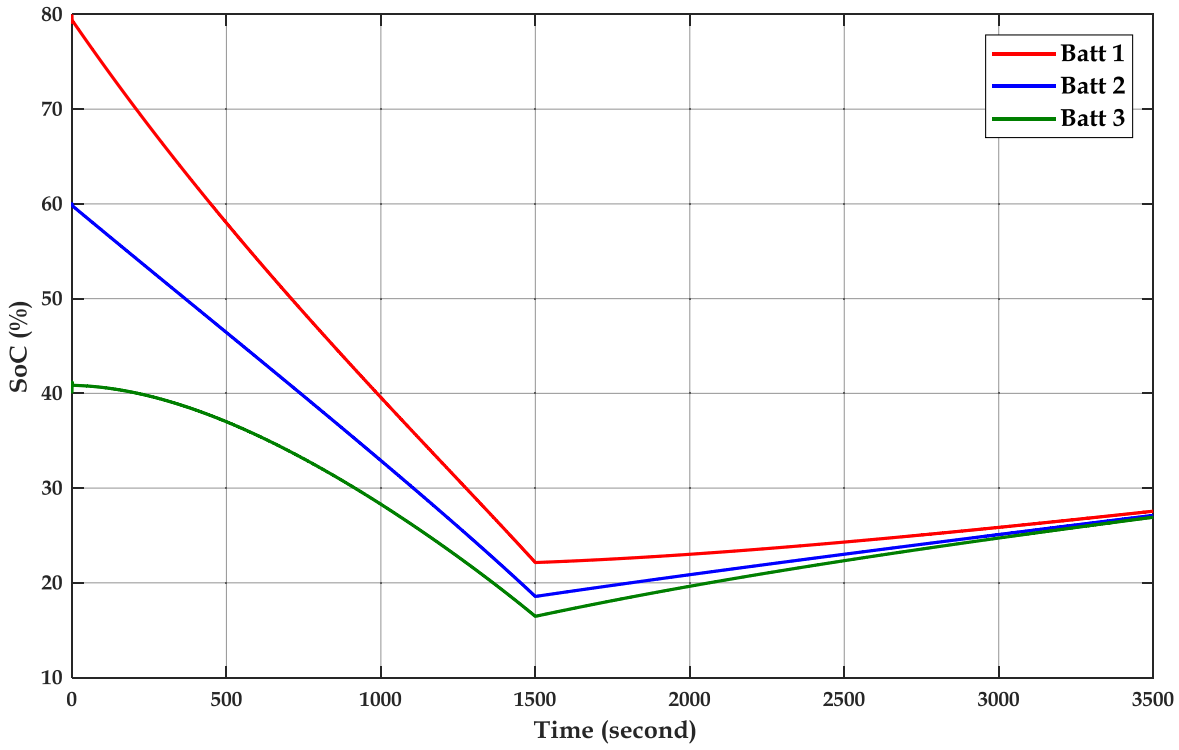

Fig. 9. SoC of three similar batteries.

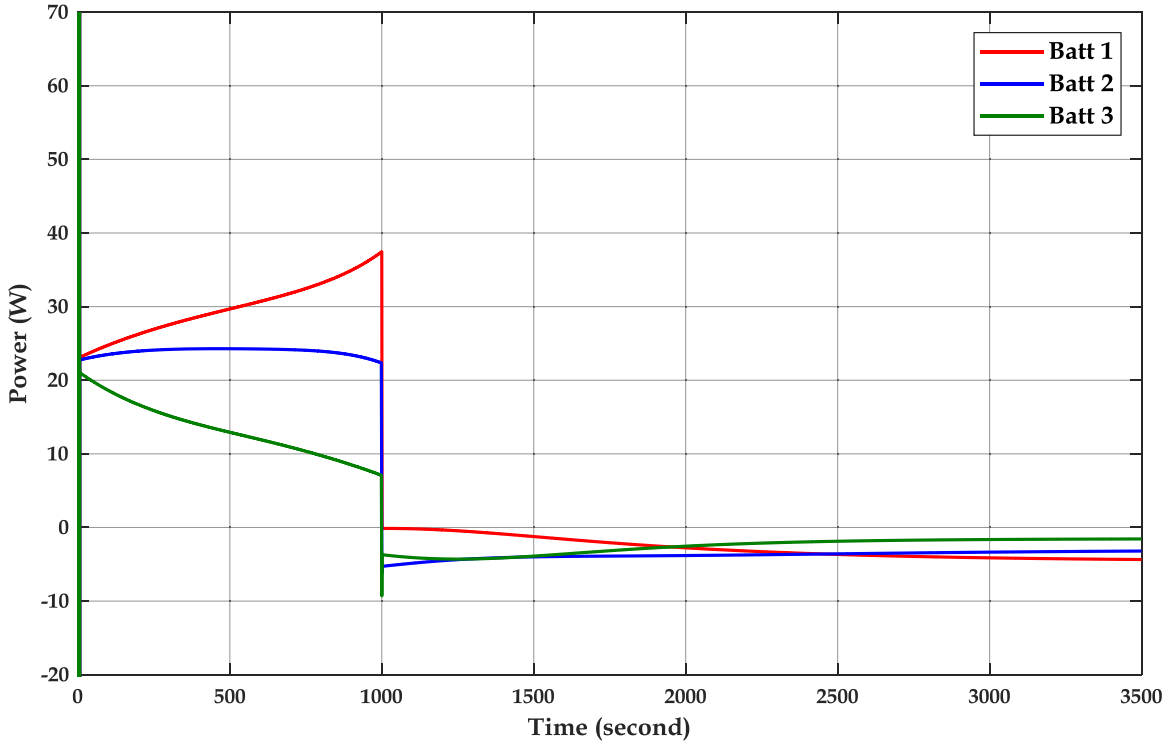

Fig. 10. Power-sharing of district batteries with similar initial SoC.

In this population, there are two types of agents: leaders and followers, the updating mechanism of the leaders are presented as

$$LP(t) = \begin{cases} TP(t-1) + c_1((ub - lb)c_2 + lb) & c_3 < 0.5 \\ TP(t-1) - c_1((ub - lb)c_2 + lb) & c_3 > 0.5 \end{cases} \quad (35)$$

$$c_1 = 2e^{-(4k/T_{\max})^2} \quad (36)$$

where LP the leaser positions at the iteration t, is c_1 and c_2 are random numbers from zero to one, T_{max} is the max number of iterations, ub and lb are the search space upper and lower boundaries and TP is the target

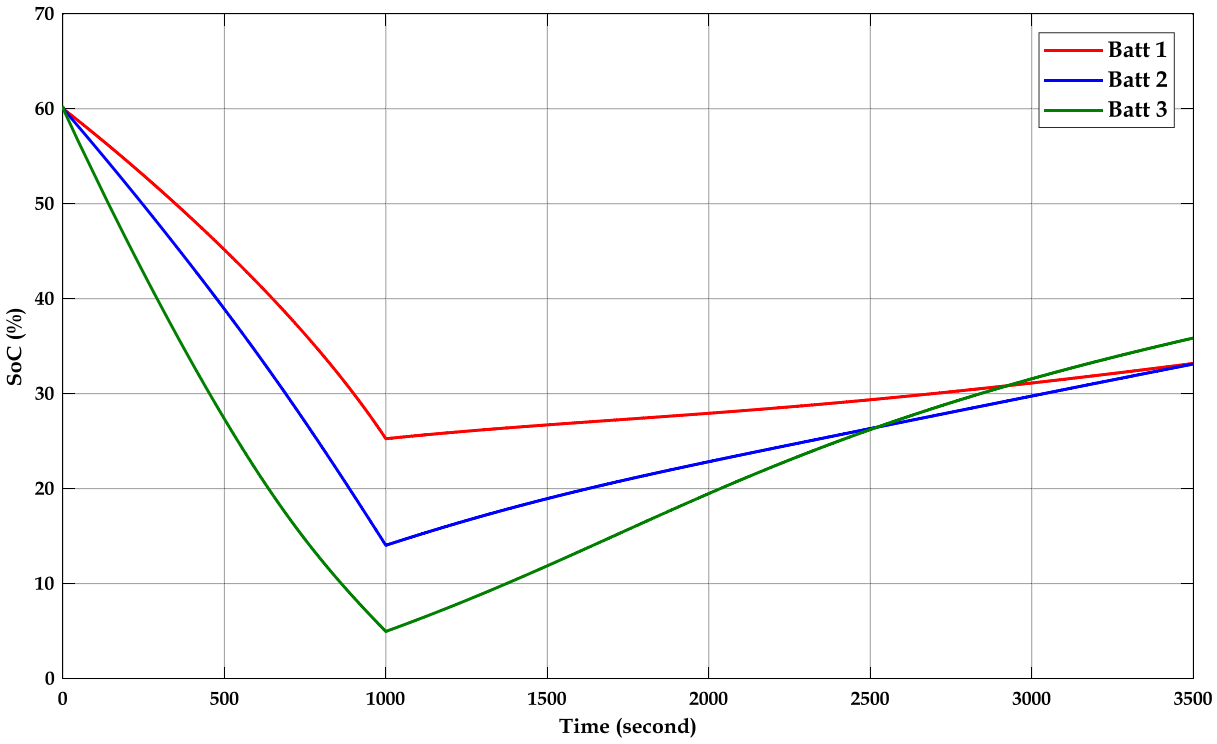

Fig. 11. SoC of three different batteries with similar initial SoC.

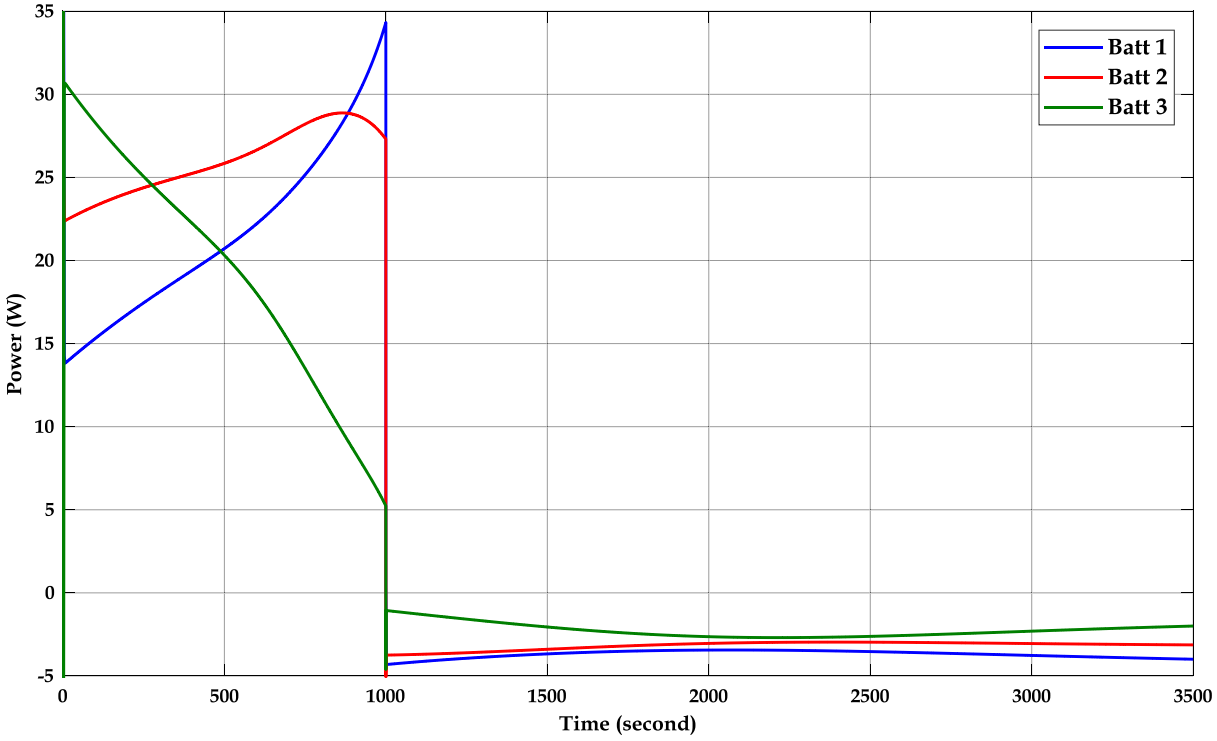

Fig. 12. Power-sharing of district batteries with different initial SoC.

position.

Each follower update his position (FP_i(t)) depending on the position of the previous agent and his previous position as

$$FP_i(t) = 0.5(FP_i(t-1) + FP_{i-1}(t)) \tag{37}$$

The battery state observation and identification including the main steps of the SSA optimization algorithm are presented in Fig. 5.

The battery state of health (SoH) can be estimated according to the initial capacity (Q_0) and the actual capacity ($Q(t)$) as follow

$$SoH_i(t) = \frac{Q(t)}{Q_0} \tag{38}$$

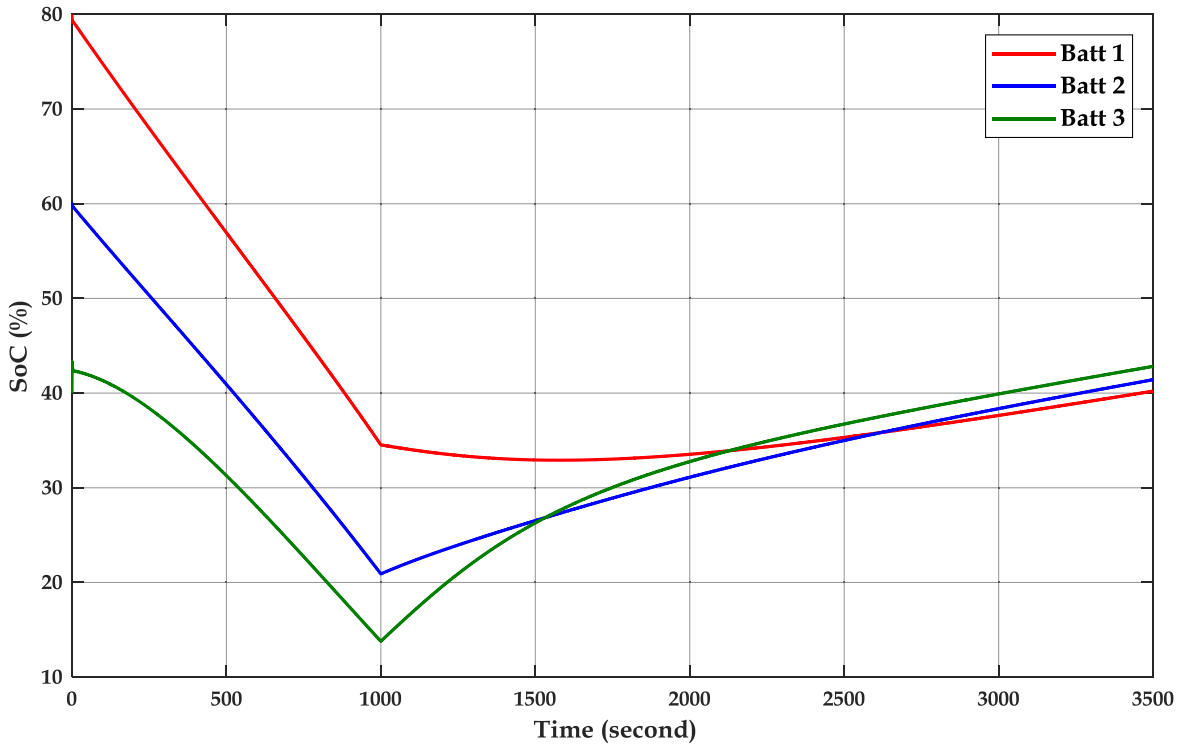

Fig. 13. SoC evolution of district batteries with different initial SoC.

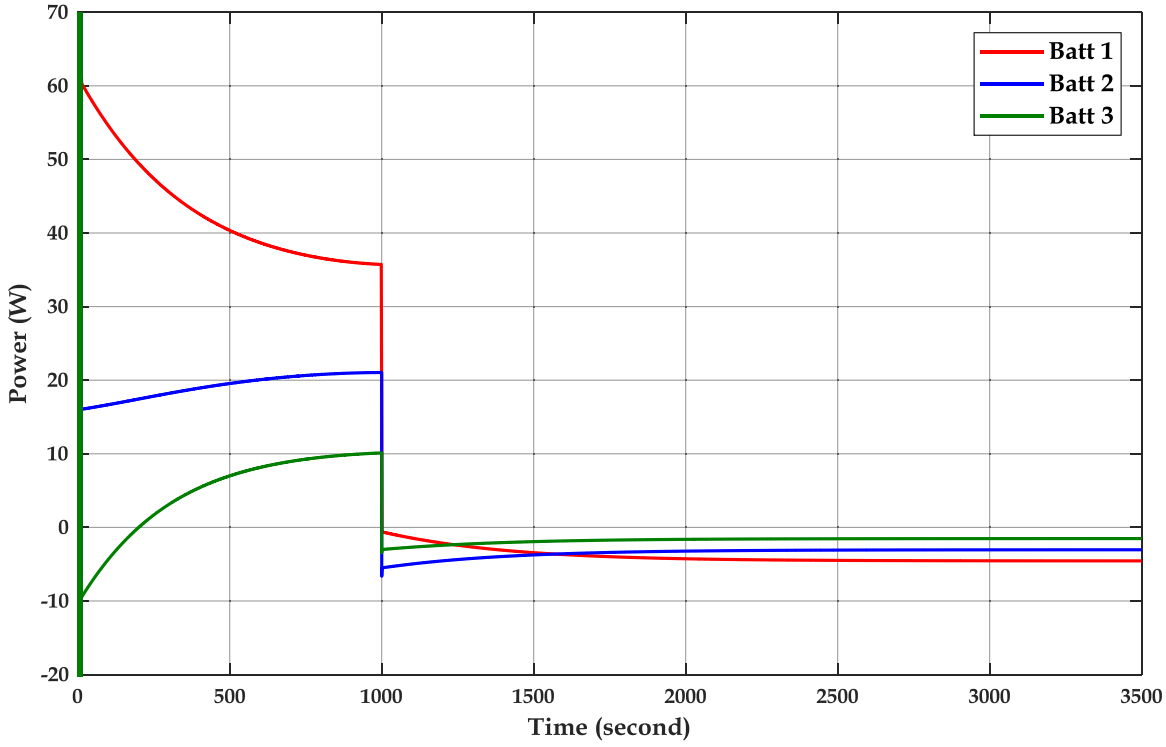

Fig. 14. Power-sharing of district batteries with adjustable virtual resistance.

The global operating scheme of the proposed control strategy including the observer and the identifier is presented in Fig. 6.

Results and Discussion

A simulation model composed of three energy storage systems (ESSs) is constructed in MATLAB/Simulink to verify and investigate the proposed strategy. Different scenarios are considered to examine the feasibility of the proposed method. These scenarios include similar and different capacities and a sudden disconnect of a battery. The system parameters are presented in Table 3.

Fig. 7 presents the load power, load current, and ESS power. The load

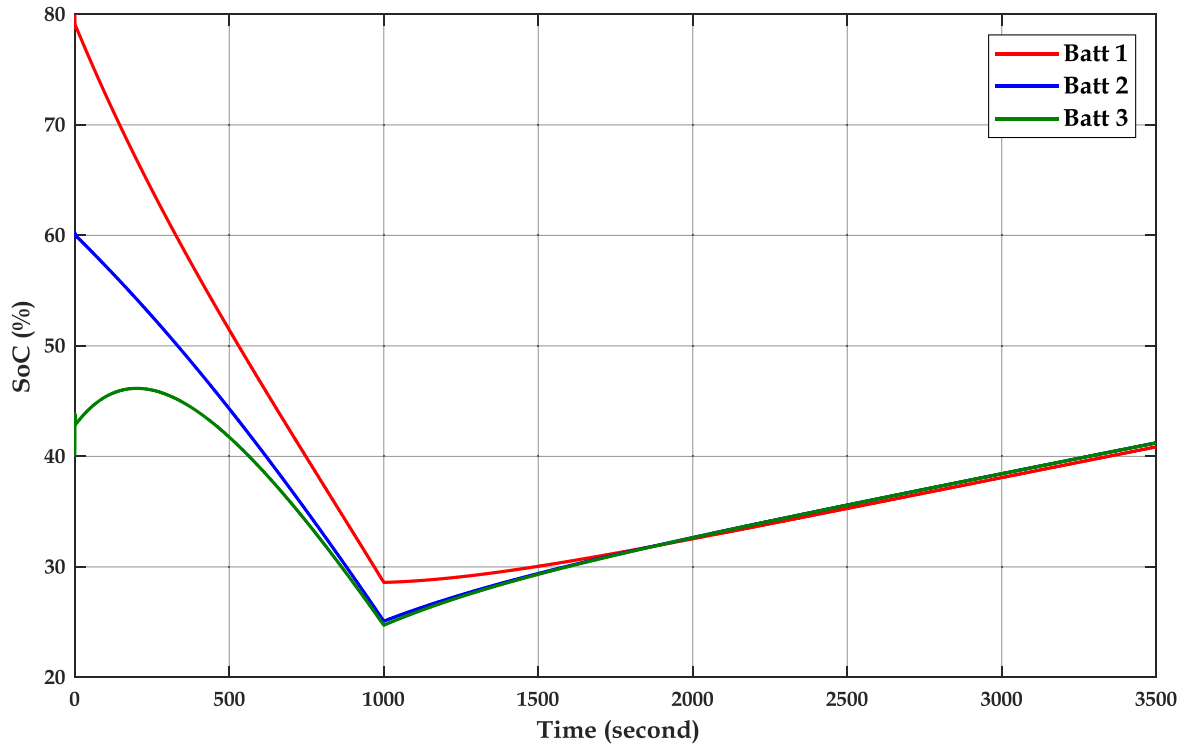

Fig. 15. SoC evolution of district batteries with adjustable virtual resistance.

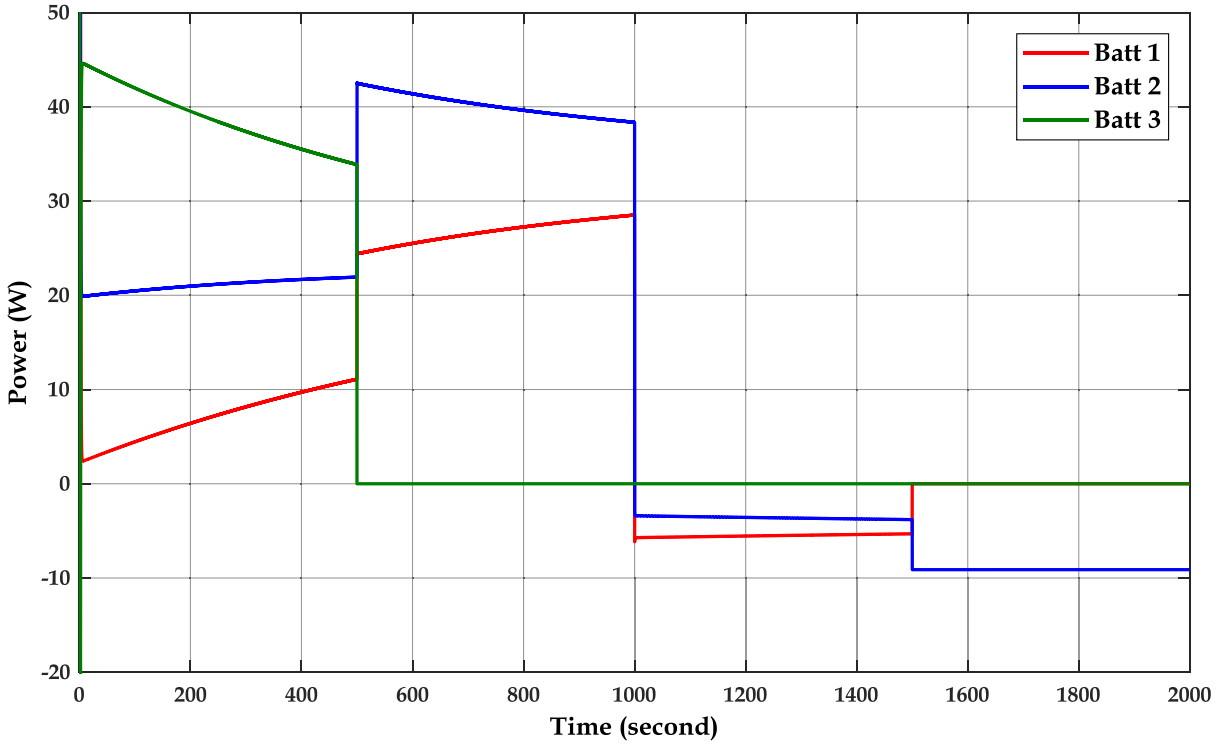

Fig. 16. Power-sharing under battery faults.

is positive and the batteries inject their power to supply the load. After 1500s, the renewable production is turned on and the load power is negative, the excess power will be stored in the ESS.

Scenario 1: Similar batteries with deferent initial SoCs

In this case, all the batteries have the same capacity (Q_{batt1}= Q_{batt2}= Q_{batt3}=1500 Ah) with different initial SoC (SoC_{batt1}=*80%*;SoC_{batt2}=60%; SoC_{batt3}=40%).

Fig. 8 presents the sharing power curves of the three considered

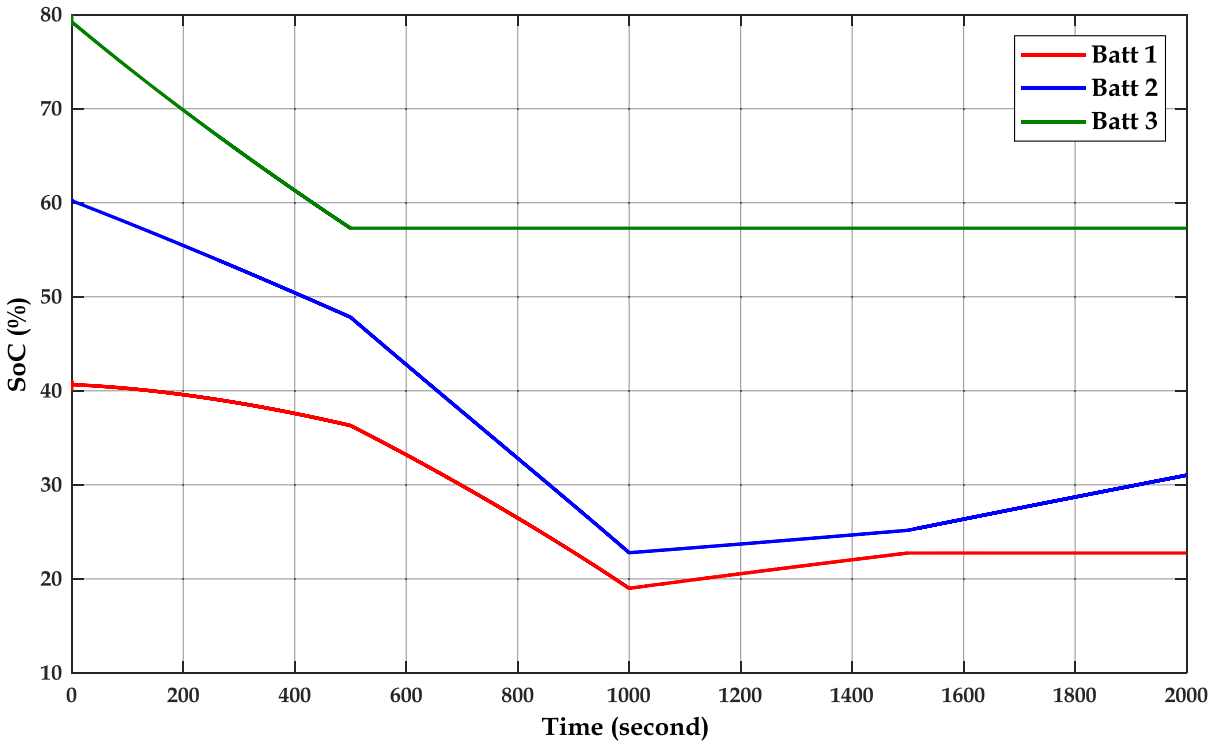

Fig. 17. SoC under battery faults.

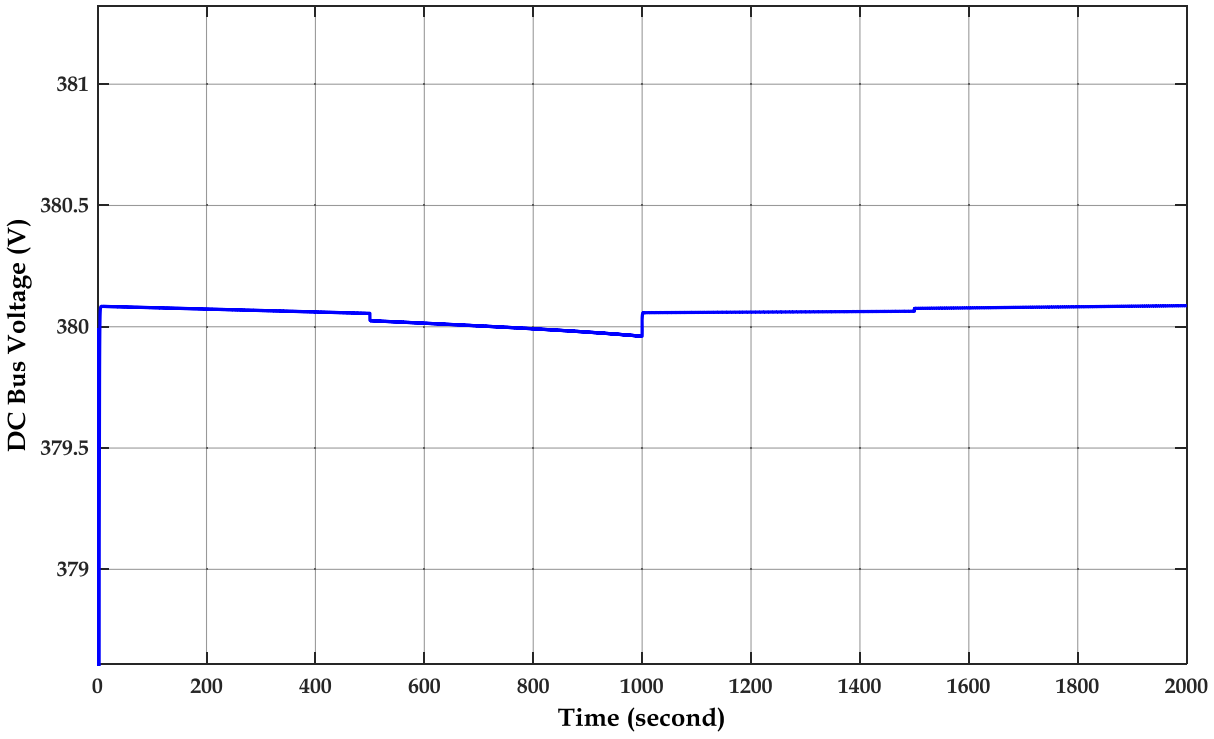

Fig. 18. DC Bus Voltage under battery faults.

batteries. Battery 1 has the higher initial SoC (80%), thus it will inject its power much higher compared with the other batteries. Meanwhile, the other batteries rise their power-sharing whereas the power of battery 1 decreases according to the converging of the SoC. After 1500s, the load power is negative and all the batteries will charge. Battery 3 which has the lower SoC will receive much power compared with the other ones.

The SoC waveforms are presented in Fig. 9. As explained in Fig. 8, battery 1 has a higher SoC with discharge much faster. At the end of the discharging period, the SoC error difference has been decreased by 25%. In the charging case, battery 3 that received higher power, its SoC rises faster. The SoC has been balanced at the end of the charging phase.

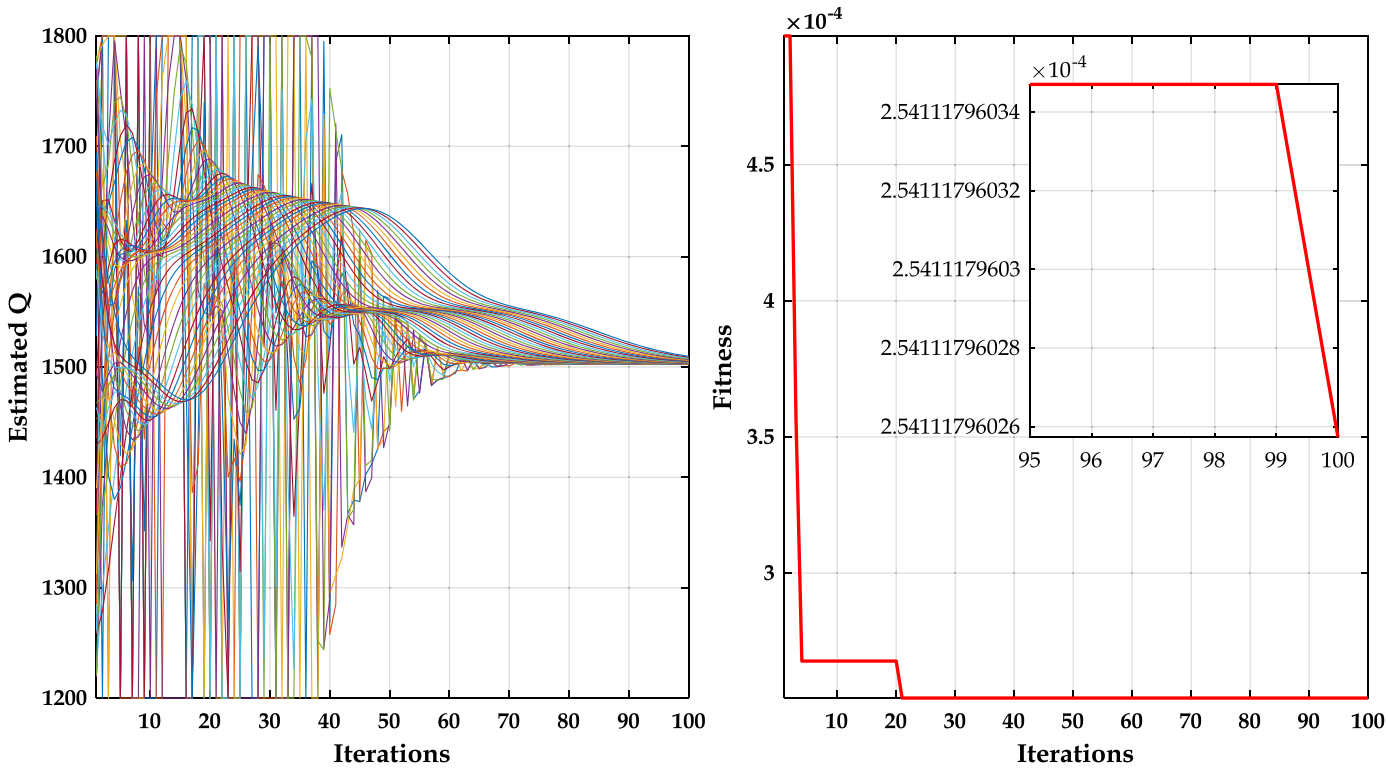

Fig. 19. Agent Evolution during the identification Process for New Battery.

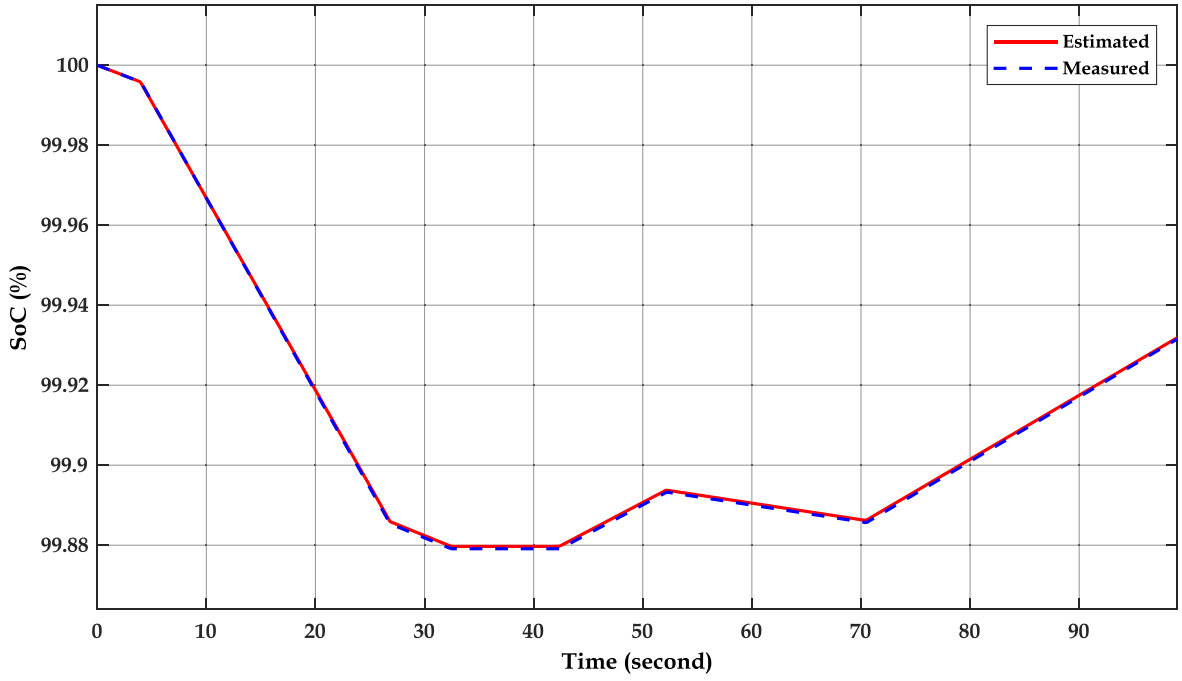

Fig. 20. Estimated and Measured SoC of a New Battery.

Scenario 2: Different batteries

Case 1: Different batteries with identical initial SoCs

In this scenario, all the batteries have the same initial SoC (60%) with deferent capacity (Q_{batt1}= 1500 Ag; Q_{batt2}= 1000 Ah; Q_{batt3}=500 Ah), the vertical resistance is set as the first case (R_1=R_2=R_3=R=0.1Ω). The power-sharing is controller using a conventional droop strategy that does not include the battery capacity.

Fig. 10 presented the power-sharing curves applying the conventional droop strategy. The SoC of each battery is illustrated in Fig. 11. From these results, the power-sharing is unequal due to the difference in the battery capacities. Battery 1 has a higher capacity (Q); thus, its SoC decrease slowly compared with the other batteries. The same notes can be observed in the charging case, the battery with the lower capacity (battery 3) will charge faster. Hence, it will achieve its max limit before the other batteries. In this case, battery 3 can achieve its max limit

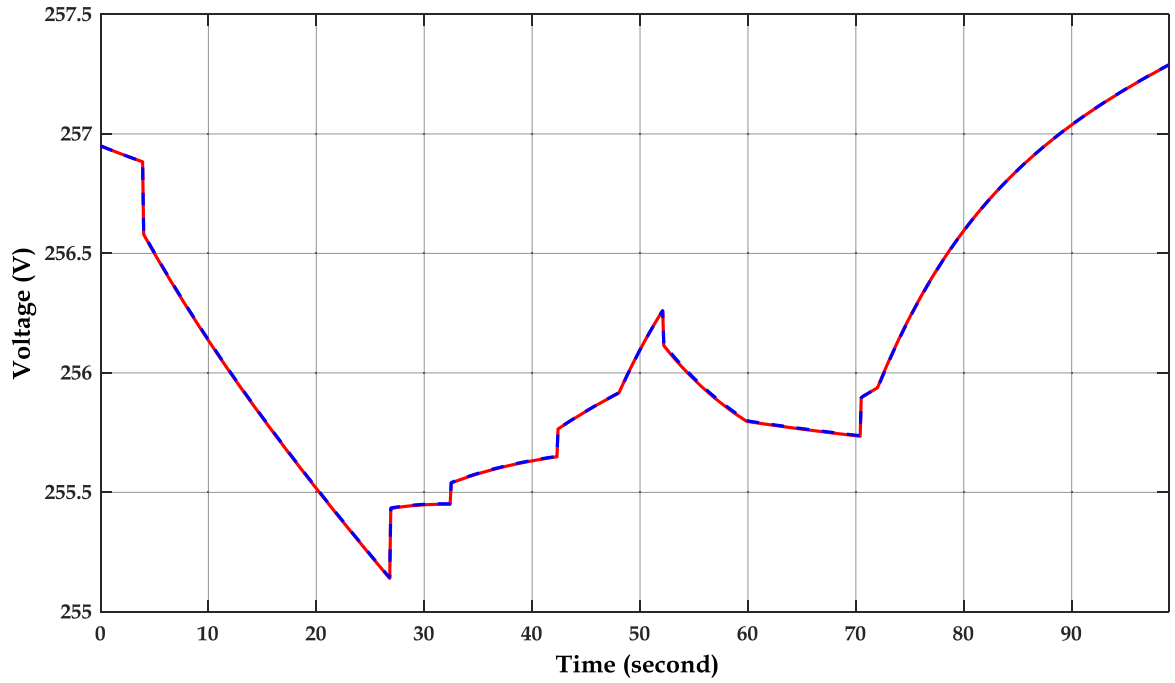

Fig. 21. Estimated and Measured Battery Voltage of a New Battery.

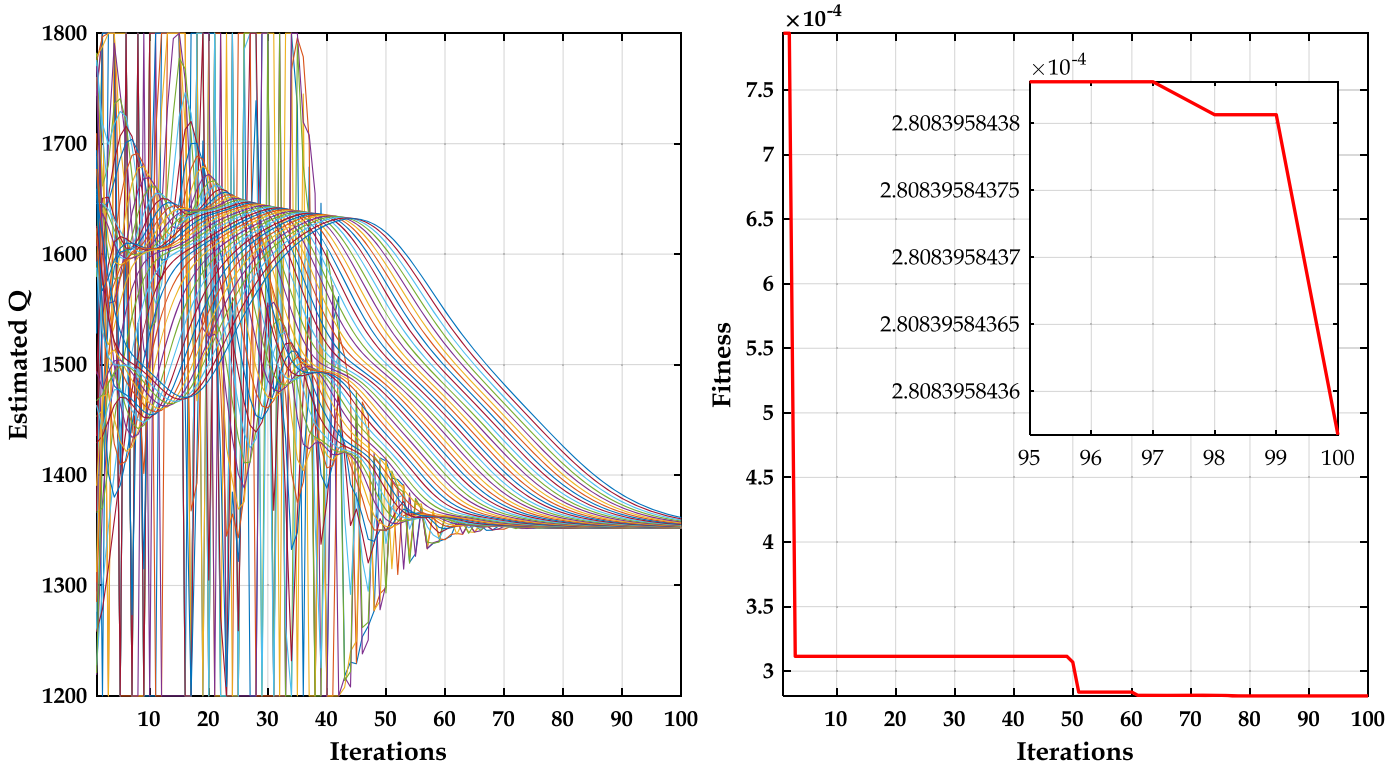

Fig. 22. Agent Evolution during the identification Process for an aged battery.

before the other batteries, and therefore, it is exposed to the overcharge risk.

Case 2: Different batteries with different initial SoCs

In this case, the batteries have different initial SoC with different capacities. The injected power and SoC variations are presented in Fig. 12 and Fig. 13 respectively. The inequality problem will reduce the lifecycle because of the overcharge or the deep discharge for the batteries that have lower capacity.

Unlike the conventional droop strategy, the adaptive droop strategy can resolve this problem by adjusting the virtual resistances as explained in Eqs (24–26), the power-sharing will be controlled as illustrated in Fig. 14.

From Fig. 14, the battery that has a higher capacity (battery 1) share the power much higher than the other batteries. The battery that has a lower capacity (battery 3) share less power to prevent the deep

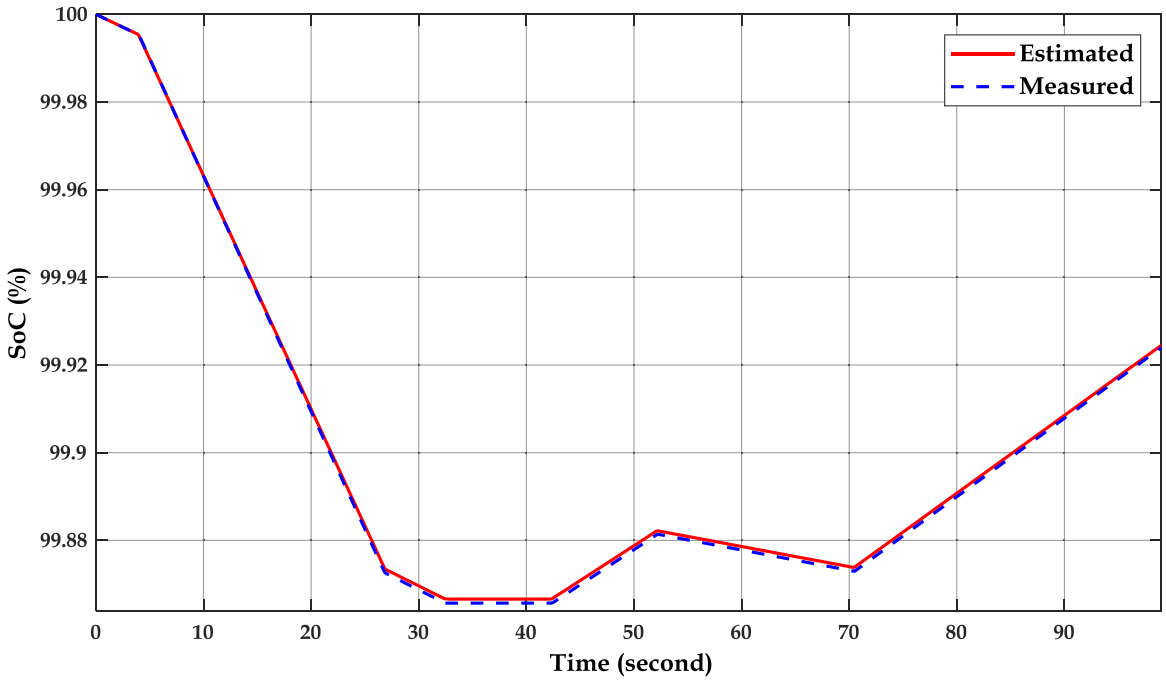

Fig. 23. Estimated and Measured SoC of an Old Battery.

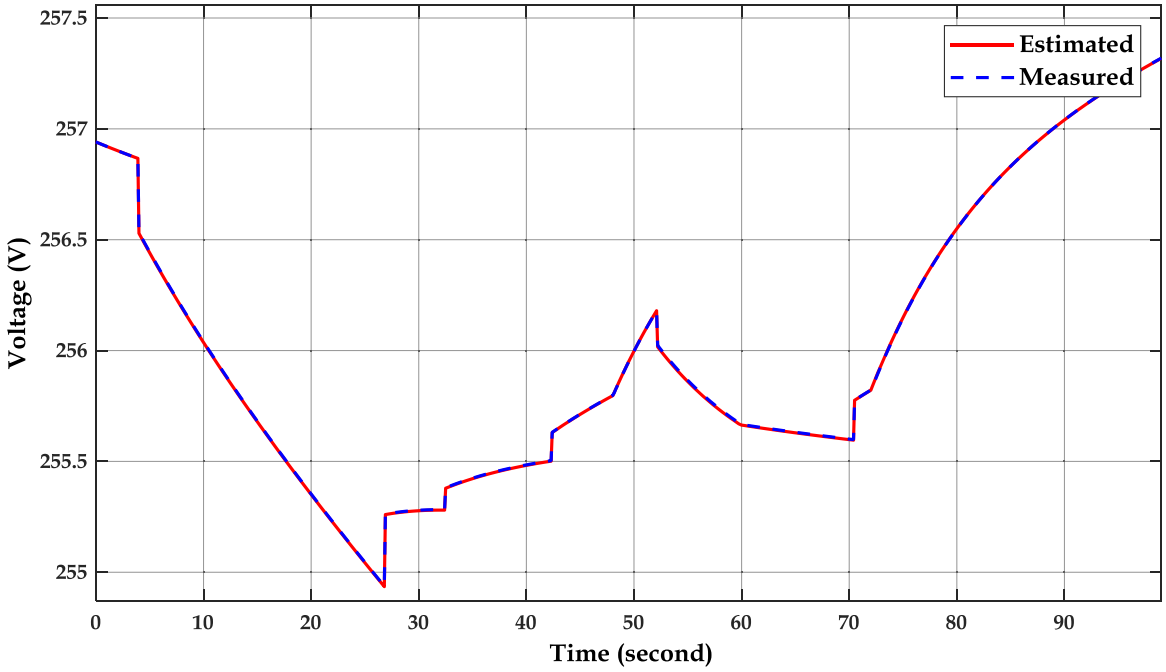

Fig. 24. Estimated and Measured Battery Voltage of an Old Battery.

discharge and to balance the SoC as illustrated in Fig. 15. The proposed strategy meet the SoC of the batteries before the end of the charging process considering the capacity of each one.

This scenario includes the battery ageing effect, where the aged battery has a lower capacity. Hence, it will share less power. The identifier allows the control system to know the existing capacity of each battery and to reconfigure the control gains according to the identifier results.

Scenario 3: Frailer of one battery

In this scenario, a robustness test will be performed. Similar batteries with different initial SoCs will be considered. During this scenario, the third battery will disconnect at t=500s, then battery 1 will disconnect at t = 1500s.

The power-sharing curves are illustrated in Fig. 16 and their SoC waveforms are presented in Fig. 17. These results can be explained as follows

- After the disconnection of battery 3 (t=500s), battery 1 and battery 2 rise their power injection to meet the load. In this instant, battery 2 still has higher SoC, therefore, it will share more power.
- After the injection of the renewable power at t=1000s, the batteries store the excess power.
- After the disconnection of battery 1 (t=1500s), battery 2 will absorb all the surplus power and ensure the power balance in the DC common bus.

Even with the disconnection of the batteries, the system voltage is still stable as illustrated in Fig. 18, which proves the robustness of the proposed droop method.

Identification of the real battery's capacity

Identification of new battery

Fig. 19 (a) illustrates the evolution of the agent positions toward the optimal solution (Q) during the identification process. Fig. 19 (a) presents the evolution of the objective function as a function of the iterations.

From this figure, the real capacity of the battery has been identified. The best agent position is 1509.69 with a precision error of 0.664%. Fig. 20 presents the curves of the real battery SoC and the estimated one, after the identification, the battery output model is similar to the battery data, the estimated voltage is also identical to the measured as presented in Fig. 21.

2- Identification of old battery:

In this case, old battery data is used, from the obtained results; the real battery is different from the initial value, and the estimated capacity is about 1353.84 where the real value is 1350 Ah. The identification error is about 0.28 %. The evolution of the agent position and the objective function during the optimization process are presented in Fig. 22 (a) and Fig. 22 (b) respectively.

The estimated data is identical to the measured battery data as illustrated, where Fig. 23 presents the SoC curves and Fig. 24 presents the estimated and battery voltage.

Conclusion and Future Work

This paper presented an optimized load-sharing approach based droop control strategy for parallel batteries applied in a DC microgrid. The fundamental purpose here is to extend the battery lifecycle by including the actual capacity in the control strategy. The proposed strategy updates the V–I curve either upwards or downwards according to the battery state of charge (SOC) and state of health (SoH) without communications between the converters. This paper proposed an estimation algorithm that estimates the battery SoH by estimating the real capacity, this last will be used to update the droop control. The estimation algorithm is based on a metaheuristic optimization algorithm called salp swarm algorithm (SSA). The power system model, the operating principle and its limitations were explained and investigated. Several operating scenarios including similar and different capacities and a sudden disconnect of a battery were simulated. The obtained results in the part of the simulation prove the ability of the proposed control strategy to handle these cases.

In future work, the combination of these control strategies with an effective energy management strategy (EMS) that handles the charge-discharge rate. The EMS is based on techno-economic objectives which tend to extend the battery SoH and meet the load with high power quality and low costs.

CRediT authorship contribution statement

Seydali Ferahtia: Conceptualization, Methodology, Software, Visualization, Investigation, Software, Validation. **Ali Djerioui:** Conceptualization, Methodology, Software, Supervision. **Hegazy Rezk:** Visualization, Investigation, Supervision, Writing – review & editing. **Aissa Chouder:** Data curation, Writing – original draft, Writing – review & editing. **Azeddine Houari:** Supervision, Writing – review & editing. **Mohamed Machmoum:** Writing – review & editing.

Declaration of Competing Interest

The authors declare that they have no known competing financial interests or personal relationships that could have appeared to influence the work reported in this paper.

References

[1] J Lacap, JW Park, L. Beslow, Development and Demonstration of Microgrid System Utilizing Second-Life Electric Vehicle Batteries, J Energy Storage 41 (2021), 102837, https://doi.org/10.1016/j.est.2021.102837 https://doi.org/.
[2] A Jani, H Karimi, S. Jadid, Hybrid energy management for islanded networked microgrids considering battery energy storage and wasted energy, J Energy Storage 40 (2021), 102700, https://doi.org/10.1016/j.est.2021.102700 https://doi.org/.
[3] NT Mbungu, RM Naidoo, RC Bansal, V. Vahidinasab, Overview of the Optimal Smart Energy Coordination for Microgrid Applications, IEEE Access 7 (2019) 163063–163084, https://doi.org/10.1109/ACCESS.2019.2951459, https://doi.org/.
[4] B Javanmard, M Tabrizian, M Ansarian, A. Ahmarinejad, Energy management of multi-microgrids based on game theory approach in the presence of demand response programs, energy storage systems and renewable energy resources, J Energy Storage (2021), 102971, https://doi.org/10.1016/j.est.2021.102971 https://doi.org/.
[5] NT Mbungu, RC Bansal, RM Naidoo, M Bettayeb, MW Siti, M. Bipath, A dynamic energy management system using smart metering, Appl Energy 280 (2020), 115990, https://doi.org/10.1016/j.apenergy.2020.115990 https://doi.org/.
[6] J Paska, P Biczel, M. Kłos, Hybrid power systems – An effective way of utilising primary energy sources, Renew Energy 34 (2009) 2414–2421, https://doi.org/10.1016/j.renene.2009.02.018, https://doi.org/.
[7] NT Mbungu, RM Naidoo, RC Bansal, MW Siti, DH. Tungadio, An overview of renewable energy resources and grid integration for commercial building applications, J Energy Storage 29 (2020), 101385, https://doi.org/10.1016/j.est.2020.101385 https://doi.org/.
[8] M Mobarrez, S Bhattacharya, D. Fregosi, Implementation of distributed power balancing strategy with a layer of supervision in a low-voltage DC microgrid, in: IEEE Appl. Power Electron. Conf. Expo., 2017, pp. 1248–1254, https://doi.org/10.1109/APEC.2017.7930855. IEEE2017https://doi.org/.
[9] W Gu, Z Wu, R Bo, W Liu, G Zhou, W Chen, et al., Modeling, planning and optimal energy management of combined cooling, heating and power microgrid: A review, Int J Electr Power Energy Syst 54 (2014) 26–37, https://doi.org/10.1016/j.ijepes.2013.06.028, https://doi.org/.
[10] Y Zeng, Q Zhang, Y Liu, X Zhuang, X Lv, H. Wang, Distributed Secondary Control Strategy for Battery Storage System in DC Microgrid, in: IEEE 4th Int. Electr. Energy Conf., IEEE, 2021, pp. 1–7, https://doi.org/10.1109/CIEEC50170.2021.9510682, 2021https://doi.org/.
[11] Z Miao, L Xu, VR Disfani, L. Fan, An SOC-based battery management system for microgrids, IEEE Trans Smart Grid 5 (2014) 966–973, https://doi.org/10.1109/TSG.2013.2279638, https://doi.org/.
[12] X Hu, F Sun, Y. Zou, Comparison between two model-based algorithms for Li-ion battery SOC estimation in electric vehicles, Simul Model Pract Theory 34 (2013) 1–11, https://doi.org/10.1016/j.simpat.2013.01.001, https://doi.org/.
[13] Q Wu, R Guan, X Sun, Y Wang, X. Li, SoC balancing strategy for multiple energy storage units with different capacities in islanded microgrids based on droop control, IEEE J Emerg Sel Top Power Electron 6 (2018) 1932–1941, https://doi.org/10.1109/JESTPE.2018.2789481, https://doi.org/.
[14] H Yang, S Li, Q Li, W. Chen, Hierarchical distributed control for decentralized battery energy storage system based on consensus algorithm with pinning node, Prot Control Mod Power Syst 3 (2018), https://doi.org/10.1186/s41601-018-0081-5 https://doi.org/.
[15] J Kim, J Shin, C Chun, BH. Cho, Stable configuration of a li-ion series battery pack based on a screening process for improved voltage/SOC balancing, IEEE Trans Power Electron 27 (2012) 411–424, https://doi.org/10.1109/TPEL.2011.2158553, https://doi.org/.
[16] J Jiang, S Peyghami, C Coates, F. Blaabjerg, A comprehensive study on reliability performance of Photovoltaic-battery-based microgrids under different energy management strategies, J Energy Storage 43 (2021), 103051, https://doi.org/10.1016/j.est.2021.103051 https://doi.org/.
[17] R Zhang, A.V. Savkin, B. Hredzak, Centralized nonlinear switching control strategy for distributed energy storage systems communicating via a network with large time delays, J Energy Storage 41 (2021), 102834, https://doi.org/10.1016/j.est.2021.102834 https://doi.org/.
[18] J Asakura, H. Akagi, State-of-Charge (SOC)-Balancing Control of a Battery Energy Storage System Based on a Cascade PWM Converter, IEEE Trans Power Electron 24 (2009) 1628–1636, https://doi.org/10.1109/TPEL.2009.2014868, https://doi.org/.

[19] Y Guan, JC Vasquez, JM. Guerrero, Coordinated Secondary Control for Balanced Discharge Rate of Energy Storage System in Islanded AC Microgrids, IEEE Trans Ind Appl 52 (2016) 5019–5028, https://doi.org/10.1109/TIA.2016.2598724, https://doi.org/.
[20] Y Xu, Z Li, J Zhao, J. Zhang, Distributed robust control strategy of grid-connected inverters for energy storage systems' state-of-charge balancing, IEEE Trans Smart Grid 9 (2018) 5907–5917, https://doi.org/10.1109/TSG.2017.2698641, https://doi.org/.
[21] T Morstyn, M Momayyezan, B Hredzak, VG. Agelidis, Distributed Control for State-of-Charge Balancing Between the Modules of a Reconfigurable Battery Energy Storage System, IEEE Trans Power Electron 31 (2016) 7986–7995, https://doi.org/10.1109/TPEL.2015.2513777, https://doi.org/.
[22] O Palizban, K. Kauhaniemi, Distributed cooperative control of battery energy storage system in AC microgrid applications, J Energy Storage 3 (2015) 43–51, https://doi.org/10.1016/j.est.2015.08.005, https://doi.org/.
[23] X Lu, K Sun, JM Guerrero, JC Vasquez, L Huang, R. Teodorescu, SoC-based droop method for distributed energy storage in DC microgrid applications. 2012. IEEE Int. Symp. Ind. Electron., IEEE, 2012, pp. 1640–1645, https://doi.org/10.1109/ISIE.2012.6237336, https://doi.org/.
[24] Chendan Li, T Dragicevic, NL Diaz, JC Vasquez, JM. Guerrero, Voltage scheduling droop control for State-of-Charge balance of distributed energy storage in DC microgrids, 2014, IEEE Int. Energy Conf. (2014) 1310–1314, https://doi.org/10.1109/ENERGYCON.2014.6850592. https://doi.org/.
[25] NL Diaz, T Dragicevic, JC Vasquez, JM. Guerrero, Fuzzy-logic-based gain-scheduling control for state-of-charge balance of distributed energy storage systems for DC microgrids, in: IEEE Appl. Power Electron. Conf. Expo. - APEC 2014, IEEE, 2014, pp. 2171–2176, https://doi.org/10.1109/APEC.2014.6803606, 2014https://doi.org/.
[26] Z Zhang, L Zhang, L Hu, C. Huang, Active cell balancing of lithium-ion battery pack based on average state of charge, Int J Energy Res 44 (2020) 2535–2548, https://doi.org/10.1002/er.4876, https://doi.org/.
[27] T Morstyn, AV. Savkin, B Hredzak, VG. Agelidis, Multi-agent sliding mode control for state of charge balancing between battery energy storage systems distributed in a DC Microgrid, IEEE Trans Smart Grid 9 (2018) 4735–4743, https://doi.org/10.1109/TSG.2017.2668767, https://doi.org/.
[28] X Lu, K Sun, JM Guerrero, JC Vasquez, L. Huang, State-of-charge balance using adaptive droop control for distributed energy storage systems in DC microgrid applications, IEEE Trans Ind Electron 61 (2014) 2804–2815, https://doi.org/10.1109/TIE.2013.2279374, https://doi.org/.
[29] H Kakigano, Y Miura, T. Ise, Distribution voltage control for DC microgrids using fuzzy control and gain-scheduling technique, IEEE Trans Power Electron 28 (2013) 2246–2258, https://doi.org/10.1109/TPEL.2012.2217353, https://doi.org/.
[30] J Zhu, MS Dewi Darma, M Knapp, DR Sørensen, M Heere, Q Fang, et al., Investigation of lithium-ion battery degradation mechanisms by combining differential voltage analysis and alternating current impedance, J Power Sources 448 (2020), 227575, https://doi.org/10.1016/j.jpowsour.2019.227575 https://doi.org/.
[31] Z Xia, Abu Qahouq JA, State-of-Charge Balancing of Lithium-Ion Batteries with State-of-Health Awareness Capability, IEEE Trans Ind Appl 57 (2021) 673–684, https://doi.org/10.1109/TIA.2020.3029755, https://doi.org/.
[32] S Chowdhury, Bin Shaheed MN, Y Sozer, An Integrated State of Health (SOH) Balancing Method for Lithium-Ion Battery Cells, 2019, IEEE Energy Convers. Congr. Expo. (2019) 5759–5763, https://doi.org/10.1109/ECCE.2019.8912932. https://doi.org/.
[33] F Altaf, B Egardt, LJ. Mårdh, Load Management of Modular Battery Using Model Predictive Control: Thermal and State-of-Charge Balancing, IEEE Trans Control Syst Technol 25 (2016) 47–62, https://doi.org/10.1109/TCST.2016.2547980, https://doi.org/.
[34] S Ferahtia, A Djeroui, H Rezk, A Chouder, A Houari, M. Machmoum, Optimal parameter identification strategy applied to lithium-ion battery model, Int J Energy Res (2021) er.6921, https://doi.org/10.1002/er.6921, https://doi.org/.
[35] S Mirjalili, AH Gandomi, SZ Mirjalili, S Saremi, H Faris, SM. Mirjalili, Salp Swarm Algorithm: A bio-inspired optimizer for engineering design problems, Adv Eng Softw 114 (2017) 163–191, https://doi.org/10.1016/j.advengsoft.2017.07.002, https://doi.org/.
[36] O Tremblay, LA. Dessaint, Experimental validation of a battery dynamic model for EV applications, World Electr Veh J 3 (2009) 289–298, https://doi.org/10.3390/wevj3020289, https://doi.org/.
[37] MMD. Ross, A simple but comprehensive lead-acid battery model for hybrid system simulation, Proc 32nd Annu Conf Sol Energy Soc Canada (2007).
[38] H. Hinz, Comparison of lithium-ion battery models for simulating storage systems in distributed power generation, Inventions 4 (2019), https://doi.org/10.3390/inventions4030041 https://doi.org/.
[39] HJ Khasawneh, MS. Illindala, Battery cycle life balancing in a microgrid through flexible distribution of energy and storage resources, J Power Sources 261 (2014) 378–388, https://doi.org/10.1016/j.jpowsour.2014.02.043, https://doi.org/.
[40] K HUANG, Y Wang, J FENG, Research on equivalent circuit Model of Lithium-ion battery for electric vehicles. 2020 3rd World Conf, Mech. Eng. Intell. Manuf. (2020) 492–496, https://doi.org/10.1109/WCMEIM52463.2020.00109. IEEEhttps://doi.org/.
[41] FLF Marcelino, HH Sathler, WWAG Silva, TR de Oliveira, PF. Donoso-Garcia, A comparative study of Droop Compensation Functions for State-of-Charge based adaptive droop control for Distributed Energy Storage Systems, 2017 IEEE 8th Int. Symp. Power Electron. Distrib. Gener. Syst. (2017) 1–8, https://doi.org/10.1109/PEDG.2017.7972492. IEEEhttps://doi.org/.
[42] R Hu, STATE OF CHARGE BALANCING DROOP CONTROL, Michigan Technological University (2015), https://doi.org/10.37099/mtu.dc.etds/919 https://doi.org/.
[43] R Hu, WW. Weaver, Dc microgrid droop control based on battery state of charge balancing. 2016, in: IEEE Power Energy Conf Illinois, PECI 2016, 2016, https://doi.org/10.1109/PECI.2016.7459242 https://doi.org/.
[44] NS Nise, Control Systems Engineering, Wiley (2019).